Pedro José Queiroz Soares

Licenciado em Ciências da Engenharia
Electrotécnica e de Computadores

Development and Efficiency Optimizing of the Human Body Energy Converters

Dissertação para obtenção do Grau de Mestre em
Engenharia Eletrotécnica e Computadores

Orientador: Professor Doutor Stanimir Stoyanov Valtchev,
FCT-UNL

Júri:
Presidente:Prof. Doutor Arnaldo Manuel Guimarães Batista
Vogal(ais): Prof. Doutor Stanimir Stoyanov Valtchev
Prof. Doutora Anabela Monteiro Gonçalves Pronto

FACULDADE DE CIÊNCIAS E TECNOLOGIA
UNIVERSIDADE NOVA DE LISBOA

Março,2014

Development and Efficiency Optimizing of the Human Body Energy Converters

"*Wisdom is only possessed by the learning.*"

Unknown

Acknowledgements

First of all, I would like to thank my mother the one and only Teresa Januária, for all the support, patience and unconditional love that she always gave me, I am really lucky to have such a caring and devote mother, I am what I am today thanks to you, love you so much.

I would also like to thank the rest of my family that supported me, believed in me, motivated me and provided everything necessary to the completion of my degree, in special my father Francisco for his experienced advices, my brother Francisco for putting up with me all of this years, my aunt Elsa for helping me research and for cooking so deliciously, my uncle Joca for his guidance, all of this wouldn't be possible without my family, I really want take this opportunity to let you know how thankful I am for all that you done for me.

To my university colleagues and friends, Palmero, Norwat, Juleu, Cristiano, Peralta, Tó, Amaral, Myki, Broculo, Sergio and André Brigida, Micael, Miranda, Nito, Lanzudo, Bola, Joana, Spread, Pantera, Marcio, Vitor, Caxinha, Debs, Baixinho, Ricardo and Nuno Rodrigues, Tito, Lois, Canarim etc, they are so many and so great that I am unable to state them all, many hours were spent studying, working and having a lot of fun, you made this academic experience amazing, in special my best friend Diogo for all the moments and notorious adventures that marked our life together and to my brothers from another mother Guga, Pistel and Alexandre thank for all you support, I am really lucky to have you in my life.

To my supervisors Prof. Stanimir Valtchef and Prof. Valentina Vassilenko, who gave me the opportunity and the means to work in this topic, to Prof. Pamies Teixeira who made possible the creation and laboratory testing of the prototype.

To all the people that participated in the laboratory testing, thank you for your time and availability, special thanks to Catarina for her help.

Last but certainly not least, to my cousin Nuno, this work is dedicated to all of my family but especially to you, I miss you a lot and I know that you are by my side giving me strength when I most need it, may your soul rest in peace.

Abstract

Nowadays it is known that the human body is continuous source of many types of energy and the devices used for collecting energy taken from the environment also have the required capabilities for the collection of the energy produced by the Human body (HB), but very limited and with very low efficiency. Low power and high yield converters are particularly needed in these cases of collecting energy from human activity and its movements due to the small amount of energy generated this way. But this situation can be improved. Enhancing or focusing the human movements by using mechanical amplifiers applied to the piezoelectric element. By doing so the input of energy in the element increases. As such increasing its output, therefore producing more energy.

Keywords: Energy Harvesting from the Human Body, Energy Conversion, Sustainable Energy, Low Power Electronics Supply.

Resumo

Atualmente sabe-se que o corpo humano é uma contínua fonte de vários tipos de energia e os dispositivos de recolha de energia do ambiente tem capacidades de recolha de energia do corpo humano, mas muito limitadas e com o rendimento muito baixo. Os conversores de baixa potencia e alto rendimento são especialmente necessários em casos de recolha de energia a partir da atividade humana e movimentos do corpo humano devido à dimensão diminuta de energia gerada desta atividade. Mas esta situação pode ser melhorada. O reforçando ou concentrando os movimentos humanos através amplificadores mecânicos aplicados ao elemento piezoeléctrico. Ao fazer isso, a entrada de energia no elemento aumenta, consequentemente aumentando a energia à saída, produzindo assim mais energia.

Palavras Chave: Colheita de Energia do Corpo humano, Conversão de Energia, Energia Sustentável, Alimentação de Eletrónica de baixa potência.

Contents

1 Introduction 1

1.1 Motivation 1

1.2 Thesis Objectives 5

1.3 Thesis Structure 5

2 State of the Art 7

2.1 Human power as a source of energy 7

2.1.1 Energy from within 8

2.1.2 Energy from Heat 9

2.1.3 Energy from Movement 11

2.2 Conversion Techniques 28

2.2.1 Basic conversion technique 28

2.2.2 SSHI technique 29

2.2.3 SECE technique 30

2.2.4 Comparison of the techniques 31

2.3 Storage Unit 32

3 Prototype and its components 33

3.1 MFC generator 33

3.2 Mechanical device 34

3.3 Conversion Circuit 36

4 Experimental procedures 37

4.1 Biopac experiment procedure 37

4.2 Prototype experiment procedure 38

5 Experimental results and analysis 41

5.1 Biopac experiment results and analysis 41

5.2 Prototype experiment results and analysis 42

5.2.1 First attempt MFC 43

5.2.2 Second attempt MFC 46

5.2.3 Third attempt MFC 49
5.2.4 MFC attempt comparison 52
5.2.5 Cl-50 attempts and analysis 53
6 Conclusions and Future Work 54
6.1 Conclusions 54
6.2 Future Work 55
7 References 56
Appendix
Biopac Male User Data Tables
Biopac Female User Data Tables
Biopac Male performance Data Tables
Biopac Female performance Data Tables

List of Acronyms

BET	Breath Effort Transducer
DE	Dielectric Elastomers
EAP	Electro Active Polymers
EH	Energy Harvesting
EMVEH	Electromagnetic Vibration Energy Harvesting
EP	Electrostrictive Polymers
ESVEH	Electrostatic Vibration Energy Harvesting
HB	Human Body
LMMG	Liquid Metal Magneto hydrodynamics Generator
MBEH	Micro Biofuel Energy Harvester
ME	Medical Electronics
MEMS	Micro Electro Mechanical System
MFC	Macro Fiber Composite
PEE	Personal Electrical Equipments
PEG	Piezoelectric Generator
SECE	Synchronous Electric Charge Extraction
SSHI	Synchronized Switch Harvesting Technique
TEH	Thermoelectric Energy Harvesters
VEH	Vibration Energy Harvesting

List of Figures

Fig. 1.1 Rechargeable battery market by chemistry (www.PrietoBattery.com) 1
Fig. 1.2 Bateries vs EH Sources (S.Roundy,2003) 2
Fig. 1.3 Commercial and under development medical devices (www.Medtronic.com) 3
Fig. 1.4 Possible power harvested from the HB (adapted from Starner,1971) 4
Fig. 1.5 Self-powered device schema(M. Loreto,2009) 5
Fig. 2.1 Electrode reaction (Tsai,2012) 8
Fig. 2.2 TEH module (Loreto,2009) 10
Fig. 2.3 Human skin reaction to temperature (Tsai, 2012) 10
Fig. 2.4 Model of a VEH attached to the HB (Mitcheson,2010) 12
Fig. 2.5 Model of a non-inertial harvester attached to the HB (Mitcheson,2010) 13
Fig. 2.6 EMVEH models (Tan,2011) 14
Fig. 2.7 ESVEH models (Tan,2011) 15
Fig. 2.8 Diagram of Electrostatic Conversion (Mateu,2005) 15
Fig. 2.9 Piezoelectric effect
(http://resources.edb.gov.hk/physics/articleIE/smartmaterials/SmartMaterials_e.htm) 16
Fig. 2.10 Temperature effect on a piezoelectric material
(http://resources.edb.gov.hk/physics/articleIE/smartmaterials/SmartMaterials_e.htm) 17
Fig. 2.11 Piezoelectric generating modes (Cottone,2012) 18
Fig. 2.12 The heel Strike System 21
Fig. 2.13 Piezolectric polymer film 21
Fig. 2.14 Backpack energy harvester with mechanical amplification 22
Fig. 2.15 Arterial Cuff Energy harvesterr 23
Fig. 2.16 Unconventional electromagnetic energy harvester 24
Fig. 2.17 The LMMG 25
Fig. 2.18 The magnetic spring generator 25
Fig. 2.19 Dielectric elastomer system 27
Fig. 2.20 Electrostatic backknee harvester 27
Fig. 2.21 Basic conversion setup and associated waveforms (Inman,2009) 28
Fig. 2.22 SSHI parallel stetup and associated waveforms (Inman,2009) 29
Fig. 2.23 SSHI series stetup and associated waveforms (Inman,2009) 29
Fig. 2.24 SECE series stetup and associated waveforms (Inman,2009) 30
Fig. 2.25 Flyback architecture of a SECE device (Inman,2009) 31
Fig. 2.26 Comparison of the conversion techniques (Inman,2009) 31
Fig. 3.1 MFC types and element disposition (www.SmartMaterial.com) 33
Fig. 3.2 M-2814-P2 34

Fig. 3.3 First BET 34
Fig. 3.4 Second BET 35
Fig. 3.5 Ring BET 35
Fig. 3.6 CI-50 Conditioner 36
Fig. 4.1 Volunteer performing the test with SS5LB in the cycle ergometer 37
Fig. 4.2 Calibration Set 38
Fig. 4.3 Frequency Generator 39
Fig. 4.4 Shaker 39
Fig. 4.5 Oscilloscope 40
Fig. 5.1 First attempt input signal 43
Fig. 5.2 First attempt output with 1MΩ load 43
Fig. 5.3 First attempt output with 2MΩ load 43
Fig. 5.4 First attempt output with 3MΩ load 44
Fig. 5.5 First attempt output with 4MΩ load 44
Fig. 5.6 First attempt output with 5MΩ load 44
Fig. 5.7 First attempt output with 6MΩ load 44
Fig. 5.8 First attempt output with 7MΩ load 44
Fig. 5.9 First attempt output with 8MΩ load 44
Fig. 5.10 First attempt output with 9MΩ load 45
Fig. 5.11 Second attempt input signal 46
Fig. 5.12 Second attempt output with 1MΩ load 46
Fig. 5.13 Second attempt output with 2MΩ load 46
Fig. 5.14 Second attempt output with 3MΩ load 47
Fig. 5.15 Second attempt output with 4MΩ load 47
Fig. 5.16 Second attempt output with 5MΩ load 47
Fig. 5.17 Second attempt output with 6MΩ load 47
Fig. 5.18 Second attempt output with 7MΩ load 47
Fig. 5.19 Second attempt output with 8MΩ load 47
Fig. 5.20 Second attempt output with 9MΩ load 48
Fig. 5.21 Third attempt input signal 49
Fig. 5.22 Third attempt output with 1MΩ load 49
Fig. 5.23 Third attempt output with 2MΩ load 49
Fig. 5.24 Third attempt output with 3MΩ load 50
Fig. 5.25 Third attempt output with 4MΩ load 50
Fig. 5.26 Third attempt output with 5MΩ load 50
Fig. 5.27 Third attempt output with 6MΩ load 50
Fig. 5.28 Third attempt output with 7MΩ load 50
Fig. 5.29 Third attempt output with 8MΩ load 50
Fig. 5.30 Third attempt output with 9MΩ load 50
Fig. 5.31 Comparison of the MFC outputs 52

Fig. 5.32 Cl-50 attempts output 53
Fig. 6.1 Linear Technology conditioner 54

List of Tables

Table 1.1 Examples of biomedical devices and their power demand 3
Table 2.1 Reported MBEHs 8
Table 2.2 Energy and power in selected activities (adapted from Starner,2004) 9
Table 2.3 Reported TEHs 11
Table 2.4 Developed mechanical power in the HB 11
Table 2.5 Charge and voltage equations of piezoelectric modes 18
Table 2.6 Conversion techniques comparison 19
Table 2.7 Piezoelectric materials and either proprieties 20
Table 2.8 Piezoelectric human EH systems 20
Table 2.9 Magnetic materials and properties 23
Table 2.10 Electromagnetic human EH systems 24
Table 2.11 EAP properties 26
Table 2.12 Electrostatic human EH systems 27
Table 2.13 Supercapacitors versus batteries 32
Table 3.1 MFC properties (adapted from www.Smart Material.com) 34
Table 5.1 Average chest expansion 41
Table 5.2 Average respiration frequency 41
Table 5.3 Average heart rate 41
Table 5.4 Input Frequency and Amplitude 42
Table 5.5 MFC Output at 0,25 Hz 45
Table 5.6 MFC Output at 0,4 Hz 48
Table 5.7 MFC Output at 0,6 Hz 51
Table 5.8 MFC Output at 0,6 Hz 51
Table 5.9 Cl-50 Output at 0,25 Hz 53
Table 5.10 Cl-50 Output at 0,4 Hz 53
Table 5.11 Cl-50 Output at 0,6 Hz 53

1 Introduction

1.1 MOTIVATION

The evolution of technologies through the passing years has created a proliferation of electronics devices with lower volume and low power consumption, such as Micro-Electro-Mechanical-System (MEMS) actuators, wireless sensors, biomedical implants, monitoring devices, audio players, remote controllers, calculators, watches, Bluetooth headsets, mobile phones, etc).

Initially batteries as we know them have been the practical solution in solving energy supply in most portable electronic devices, thanks to their relatively high energy capacity. They could reach the power demand, but still conditioned the size and weight of the electrical device. Furthermore, batteries were unable to reach the prolonged time demand, so replacement would always be needed once the battery was depleted or exhausted from recharging.

When useful devices that attract the majority of the population become cheaper and more reachable to the common person, a huge production normally follows to meet the demand, hence an even bigger production of batteries to supply them, taking in account that a

Fig. 1.1 Rechargeable battery market by chemistry (www.PrietoBattery.com , accessed 12/09/2013)

device tends to last longer than its battery. In Fig.1.1 we can see their alarming growth tendency until 2020.

This massive battery production raises some grave issues, mainly the environmental concerns regarding the hazardous substances that chemical batteries contain, increasing difficulty in their disposal or and recycle, as these processes are quite delicate and costly, it was

and still is mandatory to work out this issue and find a more conservative and sustainable solution.

A new concept emerged over the last decades, this so called energy harvesting (EH), a way to generate electrical energy from waste ambient energy with converters, to clarify, ambient light, radio waves, temperature gradients, vibrations and other sources can be converted in to electrical energy with solid state components, taking in account that this sources are relatively weak, converters for EH have to be carefully design in order to have a high efficiency to yield the maximum energy possible, making then viable.

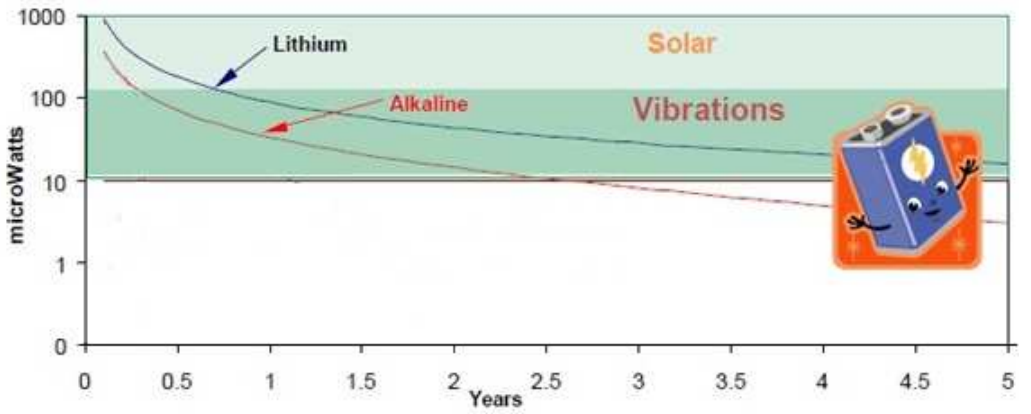

Fig. 1.2 Batteries vs EH Sources (S.Roundy,2003)

EH techniques are a great option for low power applications as life extending or even replacement for batteries, as can be seen in fig.1.2. the amount of power that can be generated by EH is low, in the milliwatt or microwatt range, but continuous, as long as the source intensity is maintained, whereas batteries tend to deteriorate and lose the initial power offer, so applications are limited but work well for low power applications that need to work much longer than the life of a typical battery. This possibility of a promising future for sensors and other small electronics, where the direct or indirect dependence of the power grid or constant replacement of battery is eliminated, has attracted a lot of interest within both the academic and industrial communities, in different areas of expertise.

Medicine is one of the many areas where EH would fit in, using MEMS based EH would be a great solution thanks to their size and also taking in consideration the low power demand of medical electronics (ME), in Table 1.1 some examples can be seen. Each year more research is done and new ME are released to the world's market, as can be see in Fig.1.3.

Table 1.1 Examples of biomedical devices and their power demand
(www.Medtronic.com, 07/08/2013)

Device	Pacemaker& cardioverter defibrillator	Hearing aid	Analogue cochlear processor	Neural Recording	Retinal stimulator	Body-area monitoring
Power	<10 µW	1-20 mW	200 µW	1-10mW	250mW	140 µW

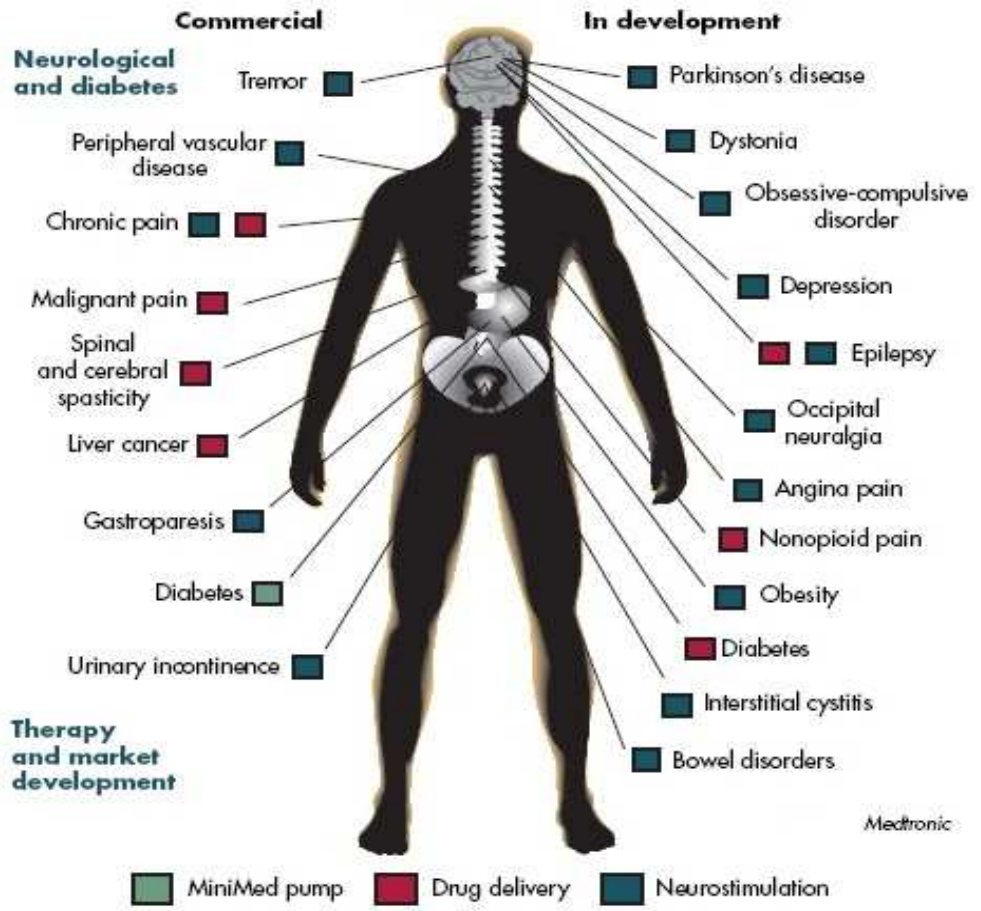

Fig. 1.3 Commercial and under development medical devices
(www.Medtronic.com, accessed 07/08/2013)

What better and closer source to supply ME than the own user, the HB is an amazing example of a source of energy that is continuously being "lost" and within the wanted range of energy, every second that we are alive our body is dissipating energy, in every step, in every breath, in every heartbeat. The human muscles, by consuming chemical energy arising from the food we eat, are able to make our body work creating mechanical energy and thermal energy, this energy may be harvested by using and adequate transduction method. As we can see in Fig.1.4 the most common source of energy of the HB and that has more available EH techniques is the kinetic energy provided from human vibrations.

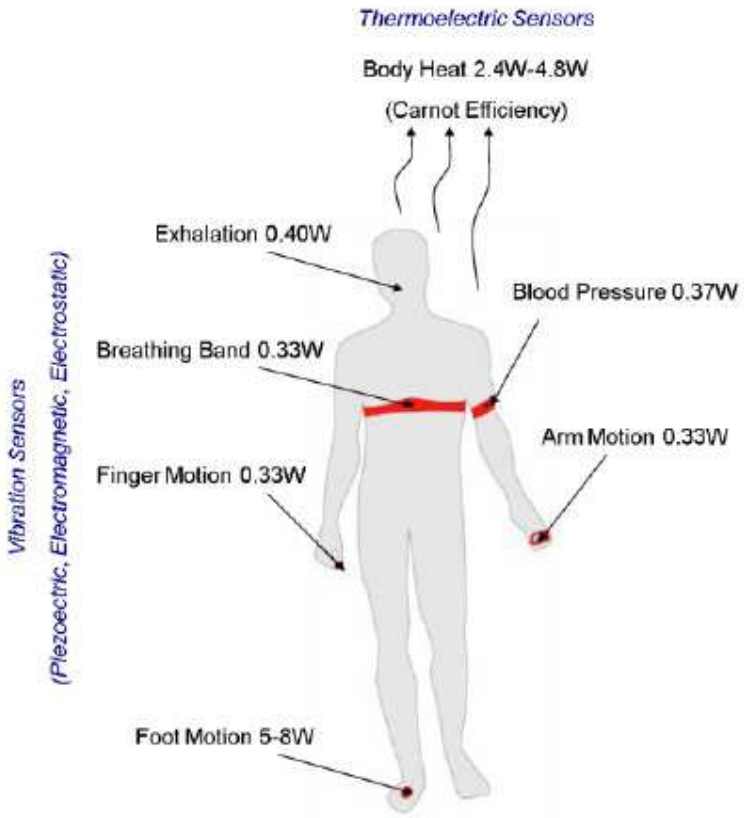

Fig. 1.4 Possible power harvested from the HB (adapted from Starner,1971)

Taking in account that human vibrations have an alternate input signal and that harvesters require a continuous and steady output to create a stable power supply. For this to occur, rectification has to be done using a AC-DC converter and voltage regulation using a DC-DC converter to keep the output as constant as possible. This is one of the most important stages of a EH device, where used devices have to be extremely efficient so their power consumption is minimal. A storage unit may or may not be used, depending on the device requirements and the source proprieties. If a bigger quantity of power is needed and if the device has no method of handling it, a storage device such as an ultra-capacitor or a rechargeable battery will be needed. Depending if it is a periodic need where a switch off mode could be used allowing energy build up in ultra-capacitor and then used when the required amount is reached. Or if it is more continuous need and the used source isn't permanent or isn't sufficient to sustain the device, a battery will be necessary. In Fig.1.5 a schema of a self powered device is presented, note this is a generic model, regardless the type of energy input so rectification may not be necessary.

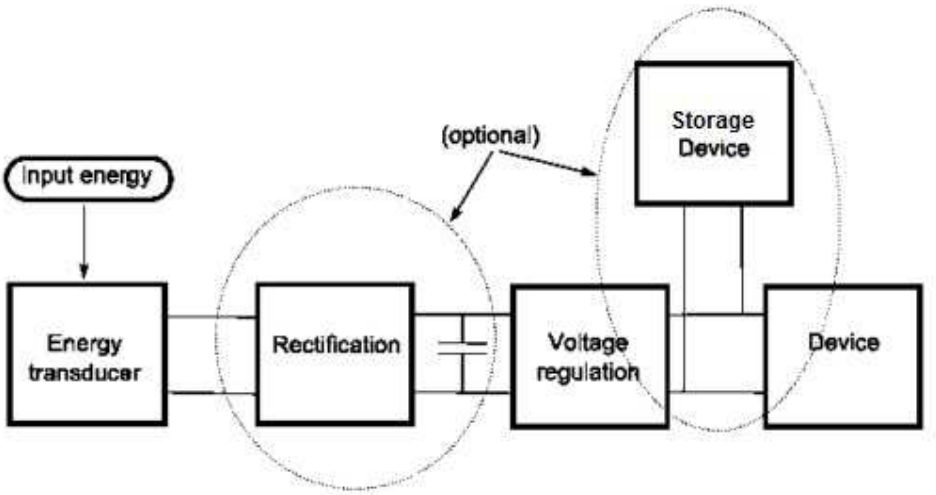

Fig. 1.5 Self-powered device schema (M. Loreto,2009)

Imagine more and more low power wearable devices being totally independent from the electrical grid and batteries thanks to EH from the human body, imagine leaving your house without even thinking if you are going to run out of battery. This is the main motivation for this thesis.

1.2 THESIS OBJECTIVES

In this thesis a study is performed about the energy that can be harvested from the HB and its associated techniques. Taking into consideration the comparative study and the previous work done by David Cavalheiro in his Breath Effort Transducer (BET) an EH prototype is created and tested and its results are presented. Performed tests and experimental results are original contributions.

1.3 THESIS STRUCTURE

This document describes the research and work developed and it organized as follows:

Chapter 1, in the Introduction the motivation, objectives and structure of the thesis are presented to the reader.

Chapter 2, in the state of the art a study of the theory behind the EH is made. Achieved values of other works are tabled and the most relevant ones are presented.

Chapter 3, in Prototype and its components the various components of Harvesting Device are described.

Chapter 4, in Experimental procedures, the Biopack experiment procedure and the prototype testing procedure are presented.

Chapter 5, in Experimental results and analysis, the Biopack experiment results and the prototype testing results are presented and analysed.

Chapter 6, summarizes the developed work and possible future work.

2 State of the Art

The exponential growth of low power Personal Electrical Equipments (PEE) and their battery dependence turned the HB into a very attractive power source. New and reliable independent ways of power supplying PEE and other electrical devices have been research over the last decades. Creating electric generators that feed unnoticeably on the renewable energy created by the HB. Replacing or largely decreasing the use of batteries and the dependence of electrical grids can be one of most important steps given by mankind in the direction of a sustainable more nature friendly world in regards to PEE's.

The research starts in section 2.1 by describing the various energies the HB produces and the known techniques of harvesting them. Before the harvested energy can properly used to supply any electrical device it was to be attuned to the required power input. In section 2.2 some conversion techniques are presented and then compared. In Section 2.3 a brief discussion on whether the use or not of a storage unit.

2.1 HUMAN POWER AS A SOURCE OF ENERGY

The evolutionary process of the human race has developed the muscles, which basically are the motors of the HB. Muscles convert chemical energy into mechanical energy with an efficiency that rounds 25. In this process thermal energy is also produced. By doing so our muscles keep us alive i.e., they make us move, pull oxygen into our system, pump blood into veins and increase our body temperature. The muscles are the creators of all biomechanical energy in the HB (Donelan,2009).

The idea of extracting energy from the HB is based on the fact that a person of 68Kg with 15% body fat, approximately stores chemical energy up to 384 MJ, and this stored energy in average is consumed at the rate of 10,7 MJ per day equivalent to only 280g of body fat, having a specific energy of 37kJ/g. Quantity of energy correspondent 800 AA batteries (2500 mAh), that weight around 20KG, which is 70 times more. Which is almost the specific energy of crude oil, 42kJ/g, is almost unbelievable the amount of energy that HB can store (Riemer,2009; Starner,2004).

The HB can be seen as a reservoir of energy that never stops leaking, it in an active way or in a passive way. Active when the action that generates energy is intentional and passive when it is and unintentional. Energy that can be transformed in to electricity using the correct EH method depending on the type of energy in question. In this warehouse one has three main options as energy source: Chemical energy that can be found inside the HB in endogenous substances that can be used as fuel for micro implantable fuel cells; Thermal energy that can be harvest through thermoelectric generators using temperature gradients; Kinetic energy that is the most readily and available type of energy that the HB has to offer, it can be converted using

three types of transducers: piezoelectric, electrostatic and inductive. These transducers can be inertial and non-inertial (Tsai,2012).

2.1.1 Energy from within

There are substances within the HB that can be used as fuel for Micro-biofuel energy harvesters (MBEH) to generate electrical energy through chemical reactions. Glucose is the most common of these substances to be considered as the fuel for implantable fuel cells. Through the oxidation of glucose, showed in Fig. 2.1, electrons are release, flowing from the anode to the cathode creating an electrical current.

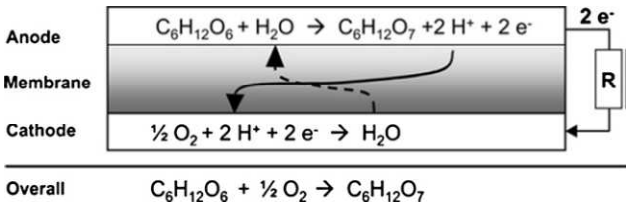

Fig. 2.1 Electrode reaction (Tsai,2012)

Few MBEH have been reported in the last years shown in Table 2.1 (adapted from Tsai,2012). They are an amazing option to power implantable ME, due their continuous power output and biocompatibility [4].

Table 2.1 Reported MBEHs (adapted from (Tsai, 2012)

$Pd_{max}(\mu W/cm^2)$	Material of electrodes	Material of substrate	Bio-fuel	Y
26	Au	PDMS/glass	ABTS	2007
20.4	Carbon	PDMS/glass	Nafion/enzyme	2005
40	Carbon nano tube	Si	Glucose oxidade	2006
100	Polymer electrolyte	N/A	Glucose	2005

2.1.2 Energy from Heat

Taking in account that the conversion of energy in muscles is around 25% efficient, means that most of the used energy is dissipated in form of heat, Table shows 2.2 the combined energy and power dissipated in daily and biologic activities.

Table 2.2 Energy and power in selected activities (adapted from Starner,2004)

Activity	Kilocal/hr	Watts
Sleeping	70	81
Lying quietly	80	93
Sitting	100	116
Standing at ease	110	128
Conversation	110	128
Eating a meal	110	128
Strolling	140	163
Driving a car	140	163
Playing piano	140	163
Housekeeping	150	175
Carpentry	230	268
Hiking, 4mph	350	407
Swimming	500	582
Mountain climbing	600	698
Long-distance running	900	1048
Sprinting	1400	1630
Exhalation	0,34	0,4
Breathing band	0,36	0,42
Finger Motion	0,002	0,0021
Blood Pressure	0,32	0,37
Arm motion	0,28	0,33
Footfalls	7,13	8,3

Energy dissipated in this way may be scavenged using Thermoelectric energy harvesters (TEH) that essentially are made of a thermocouple, a p-type semiconductor thermally connected in parallel to a n-type semiconductor and connected electrically in series as showed in Fig.2.2.

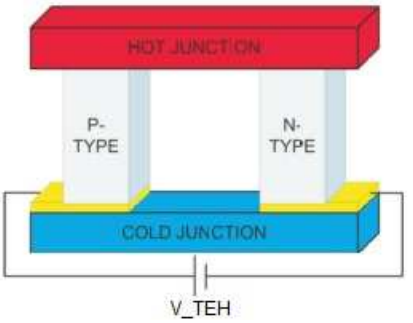

Fig. 2.2 TEH module (Loreto,2009)

These harvesters are based on the Seebeck effect, produced electrical current is proportional to thermal gradient between the hot junction in contact with the HB and the cold junction in contact with the environment. The Carnot efficiency sets an upper limit to maximum recoverable power, assuming that the HB temperature is (310K, 37ºC) and the environment (293K, 20ºC) (Starner,2004):

$$\frac{T_{body}-T_{ambient}}{T_{body}} = \frac{(310K-293K)}{310K} * 100\% = 5.5\% \quad (2.1)$$

As the ambient temperature increases this value decreases. Considering a person that is just standing at ease, a power of 128W is available checking the table 2.2, so using the Carnot method to calculate the recoverable energy leads to a value of 7.04W at 20°C.

As closer as these temperatures are, the temperature gradient is smaller and the maximum achievable power drops. Analysing the reaction of the human skin temperature regarding the surrounding temperature seen in Fig. 2.2, the location of the TEH in the HB has to be carefully chosen in order to maximize its power output (Leonov,2013).

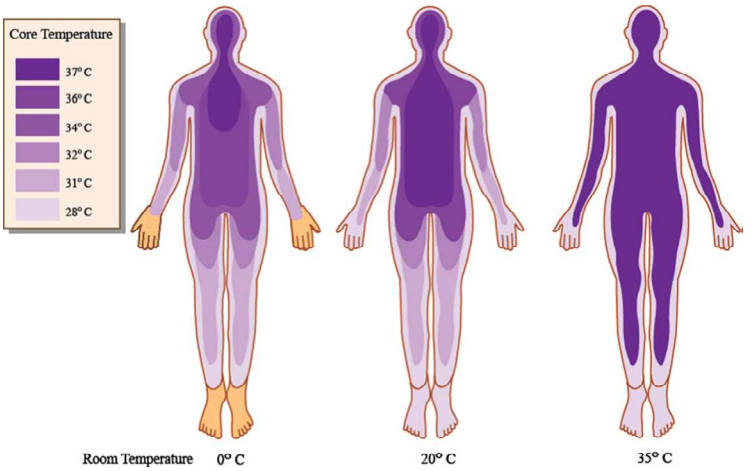

Fig. 2.3 Human skin reaction to temperature (Tsai, 2012)

The maximum power produce by a TEH is given by:

$$P_{max} = \frac{ZW^2R_{tp}}{4} \quad (2.2)$$

P_{max} being maximum power on electrically matched load, Z the thermoelectric figure of merit, $Z=S^2\sigma/k$, where S is the Seebeck coefficient, σ the electrical conductivity and k the thermal conductivity, W the heat flow that passes the thermopile, $W=\Delta T/R_{tp}$, where ΔT is the temperature difference in the thermopile and R_{tp} the thermal resistance at maximum power (Leonov,2013).

In Table 2.3 we can see some TEH for the human body that were release in the last years.

Table 2.3 Reported TEHs

P_{max}(μW)	Material	ΔT(ºC)	Y/R
100[a]	Poly-Si/Ge	12	2005/(Tsai,2012)
1-2[a]	Poly-Si/Ge	10-15	2007/(Wang,2007)
9,22[a]	Bi/Sb/Te/Se	5	2009/(Tsai,2012)
540	N/A	17	2013/(Leonov,2013)
500	N/A	17	2013/(Leonov,2013)

[a]-MEMS based.

2.1.3 Energy from Movement

The most abundant and readily available source of energy in the HB is energy that comes from movement. Each movement that we make, contracting our muscles, develop mechanical power. Some examples are shown in Table 2.4 (adapted from Cavalheiro, 2011).

Table 2.4 Developed mechanical power in the HB

Movement	**Fingers**	**Breath**	**Blood flow**	**Exhalation**	**Arms**	**Walking**
Mechanical Power(mW)	6,9-19,0	830	930	1000	3000	67000

The produced mechanical energy in the HB can be converted to electrical energy using three type of transducers, that will analysed later in this thesis: inductive, electrostatic and piezoelectric. There are two distinct methods of conversion using these transducers, the inertial and the non-inertial method.

In the inertial method a Vibration Energy Harvester (VEH), Fig 2,4(adapted from Mitcheson, 2010) is attached to the HB producing energy through the displacement or vibration of a proof mass in spring-mass system, the energy obtained is directly reliant on the mass value. The motion of the mass is described in equation (2.3), where x, y, d_t, k, m represent respectively the movement of the mass, the movement of the body, the total damping coefficient regarding the sum of all damping done in the system, the elastic constant of the spring and the mass (Cottone,2012).

$$m\ddot{x}(t) + (d_t)\dot{x}(t)\phi + kx(t) = -m\ddot{y}(t) \quad (2.3)$$

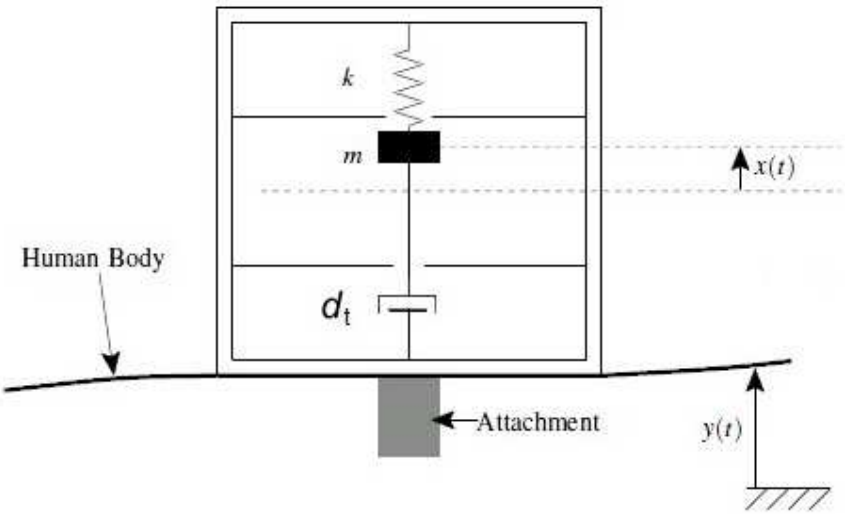

Fig. 2.4 Model of a VEH attached to the HB (Mitcheson,2010)

Through the Laplace transform of the motion equation, the power dissipated by total damping ratio is given in equation (2.4), where $\zeta_T, Y_{0,}\omega, \omega_n$ represent respectively the total damping ratio, the amplitude of the driving motion, angular frequency of the driving motion and the natural frequency.

$$P_{diss} = \frac{m\zeta_T Y_0^2 \left(\frac{\omega}{\omega_n}\right)^3 \omega^3}{\left[1-\left(\frac{\omega}{\omega_n}\right)^2\right]^2 + \left[2\zeta_T - \left(\frac{\omega}{\omega_n}\right)\right]^2} \tag{2.4}$$

In order to obtain maximum energy, these converters have to resonate at a particular frequency, called the resonance frequency. This is the frequency of the mechanical input source, in this case the human body motions, substituting $\omega = \omega_n$ and taking in account that the amplitude acceleration is, $A_0 = Y_0\omega_n^2$ on equation (2.4), it yields the maximum power dissipated.

$$P_{diss} = \frac{mA_0^2}{4\omega_n\zeta_T} \tag{2.5}$$

Nevertheless, when MEMS base energy harvesters are used on microelectronic devices, taking in consideration that $\omega_n = \sqrt{k/m}$, the resonance frequency increases due to the decrease of the harvester size and mass and it becomes higher than the frequencies related to the HB, where typical movement frequencies never pass 10Hz (Meng,2006).

The best way to max the power output of a motion-driven device is to increase the force and the displacement of the given device. Conversely to inertial harvesters, non-inertial harvesters have an external mechanical device that receives a force. In this case applied by the HB see in Fig.2.5, for example around a muscle that when contracting its diameter changes significantly or the displacement between two points of the body moving relative to each other.

In the mechanical device the movement of the HB is turned into elastic energy or rotation depending on the used device and through a converter is turned to electrical energy. Being non-inertial, there is no proof mass so the power limit is no longer dictated by its limited inertia, but by mechanical restrictions, the dimensions of the device and the input force through a displacement, equation (2.6) (Mitcheson,2010).

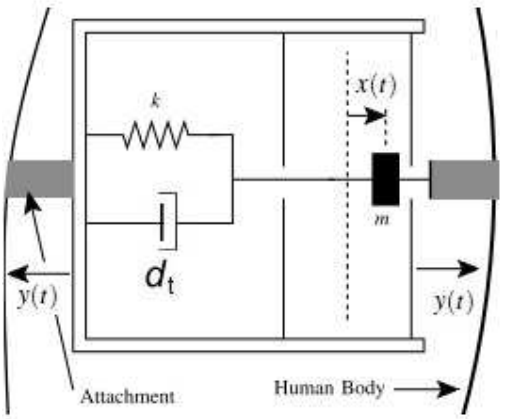

Fig. 2.5 Model of a non-inertial harvester attached to the HB (Mitcheson,2010)

$$E = \int_o^{x_0} f.dx \tag{2.6}$$

In equation 2.6, E is energy, f the applied force and x the displacement.

2.1.3.1 Mechanical energy conversion methods

When comparing all possible EH sources in the HB, the mechanical is the most potential power source in the HB and the most accessible through adopting MEMS technology.

Mechanical energy can be converted into usable electrical energy through piezoelectric, electromagnetic and electrostatic transducers. All of them can be used in mechanical energy conversion, however each one can present specific advances depending on the given situation.

2.1.3.1.1 Electromagnetic conversion

Electromagnetic conversion is based on Faraday's law, equation (2.7), which says that any magnetic flux alteration in the surroundings of a closed conductor will induce a voltage, known as e.m.f. (electromotive force), which is proportional to the strength of the magnetic field variation. This is verified whether the field strength changes or the conductor moves through it,

$$\varepsilon = -\frac{d\phi_m}{dt} \tag{2.7}$$

where $d\phi_m$ is the magnetic field flux variation over the surface of the electric conductor. In electromagnetic harvesters, permanent magnets are usually used to produce the magnetic field and coils as the conductors. This variation in the magnetic field strength can be generated by moving a magnet away or toward from the coil, moving the coil into or out of the magnetic field,

rotating the coil relative to the magnet. For a coil moving through a perpendicular magnetic field, the achievable voltage in open circuit is yielded by equation (2.8).

$$\mathrm{U}_{coil} = NBl\frac{dx}{dt} \tag{2.8}$$

Where N, B, l and x are respectively the number of turns in the coil, B induction, the length of a turn in the coil given by $2\pi r$ where r is the radius of the coil and the distance between the magnet and the coil.

Normally, there are two types of electromagnetic vibration energy harvesters (EMVEH) regarding the relative displacement, the movement between the magnet and the coil can be lateral, Fig.(2.6) (a), or the magnet can move in and out of the coil, Fig.(2.6) (b) (Tan,2011).

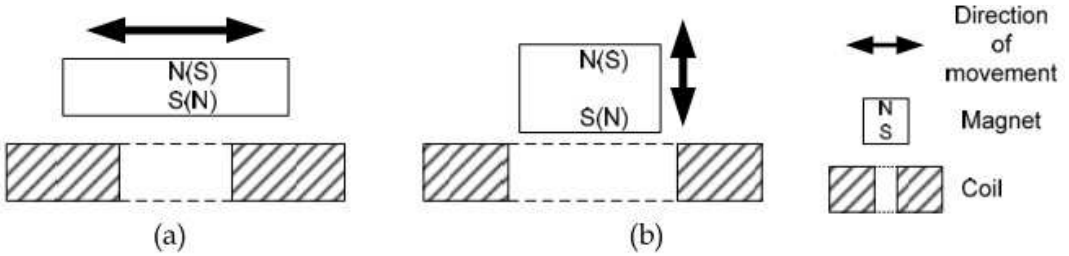

Fig. 2.6 EMVEH models (Tan,2011)

EMVEH have high output current level but a low output voltage. External voltage source isn't required and there is no need for mechanical constraints. Taking in consideration that the magnetic flux produced is yield by equation (2.9), more flux will be produced if wider area is used, as result EMVEH rely largely on their size.

$$\phi_m = \int\int_S B(s,t)dA \tag{2.9}$$

2.1.3.1.2 Electrostatic conversion

Electrostatic conversion is based on variable capacitors. Inversely to normal capacitors, one of the two electrodes sets of the variable capacitor moves, changing its capacitance equation (2.10), due to the reducing of the overlap area or to the increase of the distance between the electrode plates. There are 3 typical types of electro static vibration energy harvesters (ESVEH) shown in Fig. 2.7. There is the In-Plane Overlap which changes the overlap area of the electrodes (a), the In-Plane Gap Closing which varies distance between electrodes (b) and Out-of-Plane Gap which varies the gap between two larger electrodes (c) (Tan,2011).

$$C = \varepsilon\frac{A}{d} \tag{2.10}$$

where C is the capacitance, ε the dielectric constant of the space or material between electrodes, A the area of the plates and the d the distance between them.

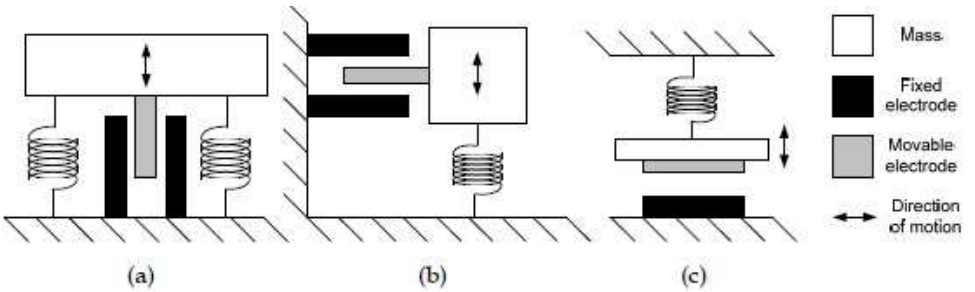

Fig. 2.7 ESVEH models (Tan,2011)

When the capacitor is charged and its movable electrode is moved against the produced electrical field, mechanical energy is converted to electrical energy. There are two different techniques of employing electrostatic conversion, constant charge or constant voltage. If a constant charge Q, is kept on the capacitor while is capacitance C, decreases, the voltage U will increase, equation (2.11).

$$U \uparrow = \frac{Q}{C \downarrow} \tag{2.11}$$

If a constant Voltage U, is maintained on capacitor while its capacitance C decreases, the charge will decrease, equation (2.12)

$$Q \downarrow = U \cdot C \downarrow \tag{2.12}$$

These conversion techniques can be better explained by looking at the diagram in Fig. 2.8, where the path ABDA refers to the constant charge technique and path ACDA to the constant voltage technique.

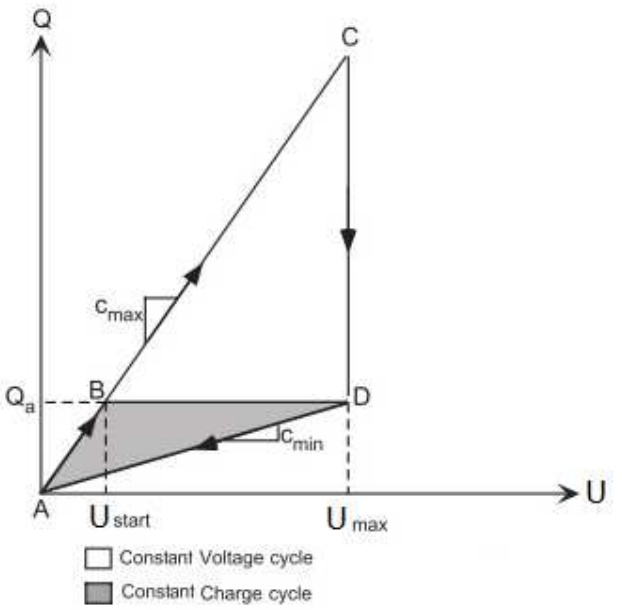

Fig. 2.8 Diagram of Electrostatic Conversion (Mateu,2005)

In both techniques the variable capacitor is only to be charged when at its maximum capacitance, that occurs in point A, for achieving maximum efficiency the precharge as to be extremely synchronized with movement that triggers the variation of the capacitance. From A to B in the constant charge technique or from A to C in the constant voltage technique the capacitor is charged to a primary voltage, U_{start} and U_{max} respectively, then as the electrode plates take apart from B to D or from C to D, the capacitance decreases from C_{max} to C_{min} and as the charge or the voltage is kept constant, the voltage increases or the charge decreases. In both these processes mechanical energy is converted into electrical energy. In both cases the path D to A represents the discharge of the capacitor. The main difference in the constant voltage technique is that a larger initial voltage is needed and there is more net energy gained, yielded by the area ACD and ABD in the constant charge, where the net energy is lower but with also lower pre-charge (Tan,2011).

ESVEH have a high voltage output and low output current. They are easy to integrate with MEMS technology, as the main components are variable capacitors, which are commonly used in MEMS devices. However, mechanical constraints and external voltage source or pre-charged electrodes are necessary.

2.1.3.1.3 Piezoelectric conversion

The Greek-Derived word piezoelectricity meaning ''pressure electricity'' describes an effect that was discovered in 1880 by the brothers Pierre and Jacques Curie. This effect called the direct piezoelectric effect can generate electric charge through the application of mechanical stress, and conversely, a mechanical deformation is generated when the ceramic is submitted to an electrical field, as it can be seen in Fig.2.9. This effect occurs due to the separation of electric charge in the crystal structure required to produce electric dipoles. (Tan,2011).

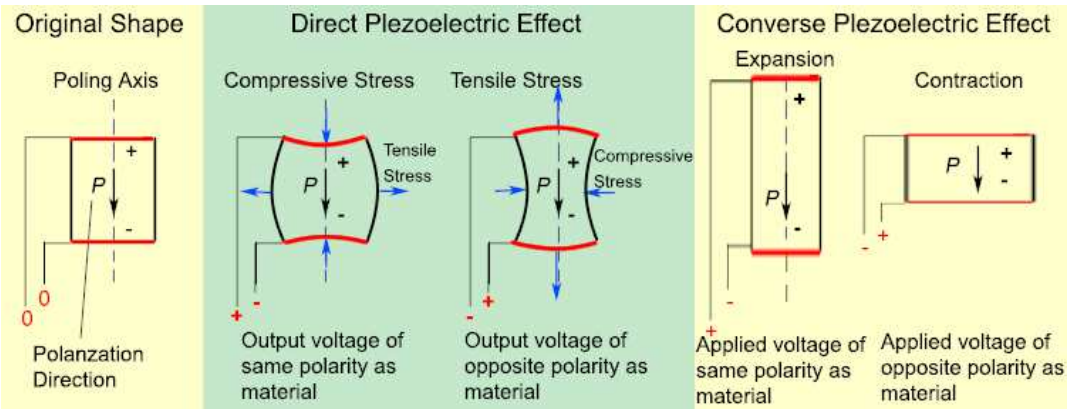

Fig. 2.9 Piezoelectric effect (http://resources.edb.gov.hk/physics/articleIE/smartmaterials/SmartMaterials_e.htm, accessed 03/04/2013)

The Curie brothers noticed that piezoelectricity is observed only in crystals with no center of symmetry because in noncrystalline materials and in the centrosymmetrical types of crystals

the charges tend to be displaced in opposite directions; therefore, pressure produces no external electrical effect in them. Crystals of low symmetry, however, have a tendency for their valence electrons to be squeezed in one direction polarizing them by doing so, furthermore, it was also observed that piezoelectricity is an anisotropic characteristic, and when a piezoelectric material is heated above his stated Curie temperature it tends to align its structure to a more symmetrical one, losing its polarization, decreasing is piezoelectric performance Fig.2.10 (Mateu,2005).

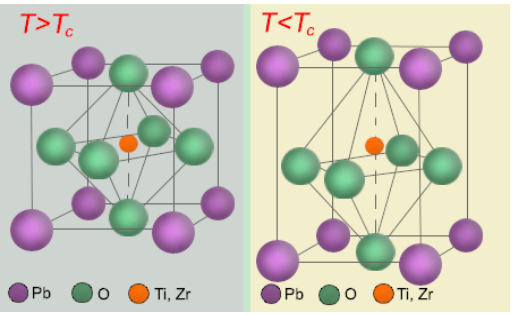

Fig. 2.10 Temperature effect on a piezoelectric material (http://resources.edb.gov.hk/physics/articleIE/smartmaterials/SmartMaterials_e.htm, accessed 03/04/2013)

The most used piezoelectric materials are the ceramics, due to the high dielectric constant that results from its polarization process and due to its high resonance frequency.

In piezoelectric materials there is a strong electromechanical interaction that can be translated in a simplified form by the equations 2.13 and 2.14.

$$D = dT + \varepsilon^T E \tag{2.13}$$

$$S = S^E T + dE \tag{2.14}$$

Where D (C/m^2) is the electric displacement, T (N/m^2) is the applied mechanical stress, S (m/m) is the mechanical strain, S^E is the mechanical strain developed when a mechanical stress is applied at a constant electric field, E (N/C) is the applied electric field, d (C/N) is the piezoelectric charge constant that represents the dielectric displacement developed when a mechanical stress is developed and ε^T the dielectric permittivity of the material when submit to a constant mechanical stress.

The two more common ways of engaging a piezoelectric material into generating electric charge are the 33 mode and the 31 mode, represented in Fig. 2.11, describing the three degrees of freedom, x, y and z with 1,2 and 3.

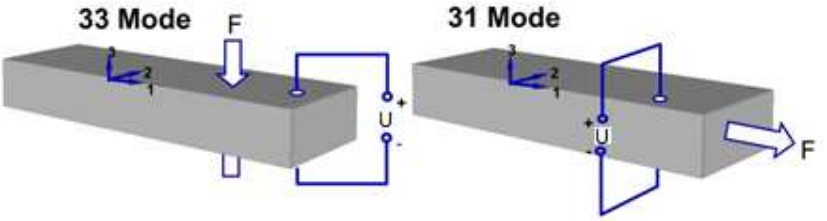

Fig. 2.11 Piezoelectric generating modes (Cottone,2012)

The voltage (U) and the charge (q) obtained by each mode is shown in Table 2.5. Where g (Vm/N) the piezoelectric voltage constant, is the electric field generated by a piezoelectric material when mechanical stress is applied, the dimensions of the piezoelectric material are given by W width, L length and H thickness, the applied force is given by F.

Table 2.5 Charge and voltage equations of piezoelectric modes (adapted from Mateu,2009)

	Mode 31	Mode 33
U	$g_{31}\frac{F_1}{W}$	$g_{33}\frac{F_3}{WL}H$
q	$d_{31}\frac{F_1 L}{H}$	$d_{33}F_3$

The first subscript to d and g indicate the direction of polarization generated, the second subscript shared by F subscript is the direction of the applied stress or the induced strain. Piezoelectric converters compared with other converters have much higher voltage levels, don't need external voltage sources to start the process and have no mechanical limitations, however they are more difficult to implement with MEMS technology, the smaller the device the less charge is generated.

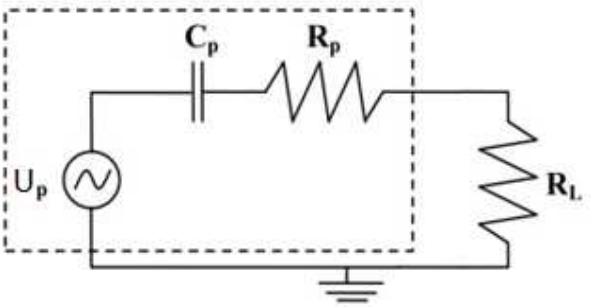

Fig. 2.12 Piezoelectric circuit model (Cottone,2012)

In Fig. 2.12 an example of a piezoelectric generator (PEG) circuit is presented. Formed by the components inside the dashed rectangle, a voltage source Up, a capacitor Cp and a resistor

Rp. The R_L load is not part of the piezoelectric circuit, but is used to calculate the generated power with equation (2.15).

$$P = \frac{U_{rms}^2}{R_L} \tag{2.15}$$

2.1.3.2 Mechanical energy conversion methods comparison

In particular, when dealing with mechanical energy scavenging, many studies are considered, by analysing each method advantages and disadvantages in Table 2.6 (adapted from F.Cottone, 2012), a better awareness of the mechanical conversions methods can be reach and conclusions can be taken.

Table 2.6 Conversion techniques comparison

Type	Advantages	Disadvantages
Electromagnetic	-no need of smart material -no external voltage source	-bulky size: magnets plus coils -difficult to integrate with MEMS -max voltage of 0,1V
Electrostatic	-no need of smart material -compatible with MEMS -voltages of 2~10V	-external voltage source need -mechanical constraints need -capacitive
Piezoelectric	-no external voltage source -high voltages of 2~10V -compact configuration -high coupling in single crystals	-depolarization -brittleness -charge leakage -high output impedance

The more significant disadvantages are present by the electromagnetic and the electrostatic methods, the bulky size and the need for external voltage source respectively. The piezoelectric conversion method is considered the potential choice when compared with electromagnetic and electrostatic conversion due to the high energy density that the piezoelectric materials provide. Such comparison is given in table 2.7 (taken from Mickaël Lallart, 2012).

Table 2.7 Energy density comparison

Type	Energy Density (mJ cm^{-3})
Piezoelectric	35.4
Electromagnetic	24.8
Electrostatic	4

2.1.3.3 Mechanical human EH developed projects

Many projects were developed on mechanical EH harvesting in the last decades, using difference approaches and materials depending on the conversion technique and on the used input source. In the next sections the used materials and some relevant projects on Human EH using each conversion technique are described and analyse.

2.1.3.3.1 Piezoelectric developed projects and used material

The most common man made materials used in piezoelectric EH and in others applications such as sensors or actuators can be seen in Table 2.7 (Cottone, 2012). Barium titanate (BaTiO3) was the first piezoelectric ceramic discovered, lead zirconate titanate (Pb[ZrxTi1−x]O3) more commonly known as PZT, which is the most common piezoelectric ceramic in use today and polyvinylidene fluoride (PVDF) that exhibits piezoelectricity several times greater than quartz. Unlike ceramics, long- chain molecules attract and repel each other when an electric field is applied. This table also shows relevant proprieties of these materials in both horizontal and vertical directions and also includes their dielectric constant.

Table 2.7 Piezoelectric materials and either proprieties

Property	PZT-5H	PZT-5A	$BaTiO_3$	PVDF
d_{33} (10^{-12} C N^{-1})	593	374	149	-33
d_{31} (10^{-12} C N^{-1})	-274	-171	78	23
g_{33} (10^{-3} V m N^{-1})	19,7	24,8	14,1	330
g_{31} (10^{-3} V m N^{-1})	-9,1	-11,4	5	216
k_{33}	0,75	0,71	0,48	0,15
k_{31}	0,39	0,31	0,21	0.12
$\varepsilon/\varepsilon_0$	3400	1700	1700	12

In Table 2.8, some recent piezoelectric human EH systems are shown and then analysed.

Table 2.8 Piezoelectric human EH systems

Source	Frequency (Hz)	Average Power reported(mW)	Ref
Heel strike	1	90,3	(Howells,2009)
Footstep	1	0,00034	(Klimiec,2008)
Walking (backpack)	2,75	0,4	(Feenstra,2008)
Arterial movements	1,3	0,000016	(Potkay,2008)

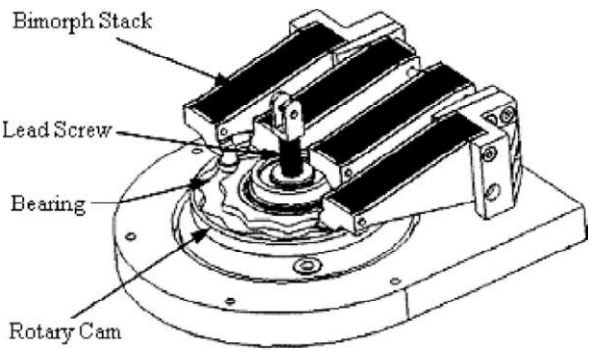

Fig. 2.12 The heel Strike System

The Heel Strike System (Howells,2009), is a system that converts mechanical strain into electrical energy using the piezoelectric effect, it is divide in two parts, the Heel Strike Generator that uses the body weight in each gait to apply stress in a lead screw and gear train, converting that stress into rotation deflecting sinusoidally four PZT-5A(Lead Zirconate Titanate) bimorph crystal stacks, each one out of phase 90º, so they absorb most of the elastic energy created this way, generating electrical charge, then the second part of the system comes in to action, a power electronics circuit that extracts, stores and regulates the electrical energy from the four phases and converts them into a output 12VDC voltage pulse. There are three main issues in this system, firstly the rotation is not entirely cancelled after each oscillation so the resulting force opposes the down force created by the user in each step, reducing the mechanical energy produce, lowering the conversion efficiency. Secondly is the locating of the system, most of the low power devices that can be supply by such generator are at waste level or even higher, rising the distance from the generator to the consuming device increases the energy lost in the transport between them and it maybe be nuisance to the user, and thirdly obviously power is only generated while walking, so whenever the user stops, the electrical energy production also stops, this can be a problem depending on the purpose of this generator.

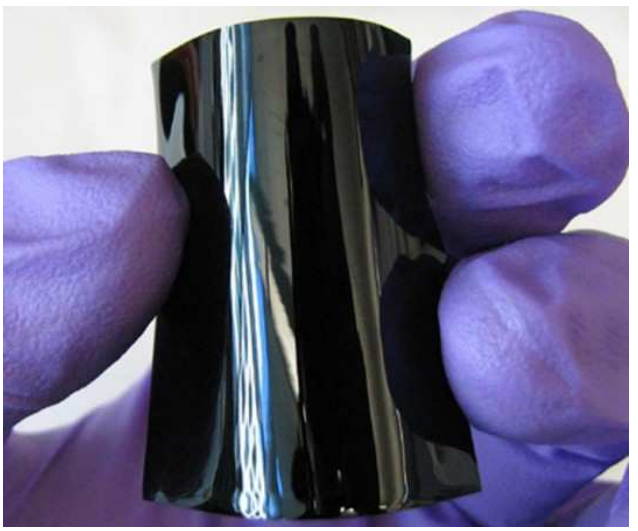

Fig. 2.13 Piezolectric polymer film

Most of the piezoelectric materials have high stiffness, making then hard to be implement in human activities without being noticeable to the user. In (Klimiec,2008) a new type of piezoelectric material is used, a extremely flexible piezoelectric polymer film is used in shoe insole, weighting only 0,1012 g a single foil generated 340 nW. Applying multilayer foils would easily increase the generated power significantly.

Fig. 2.14 Backpack energy harvester with mechanical amplification

As said before piezoelectric stacks have poor energy efficiency in harvesting applications due to their high stiffness that makes the material very difficult to strain. In (Feenstra,2008) another way is used to facilitate the straining process, using a mechanically amplified backpack energy harvester which allows the relatively low forces generated during the human walking to be transformed to high forces on the piezoelectric stack. The results show an increase of 12% in power output over the previous backpack generators without mechanical amplification, making it extremely relevant to consider the use of mechanical amplification in pressure based PEGs.

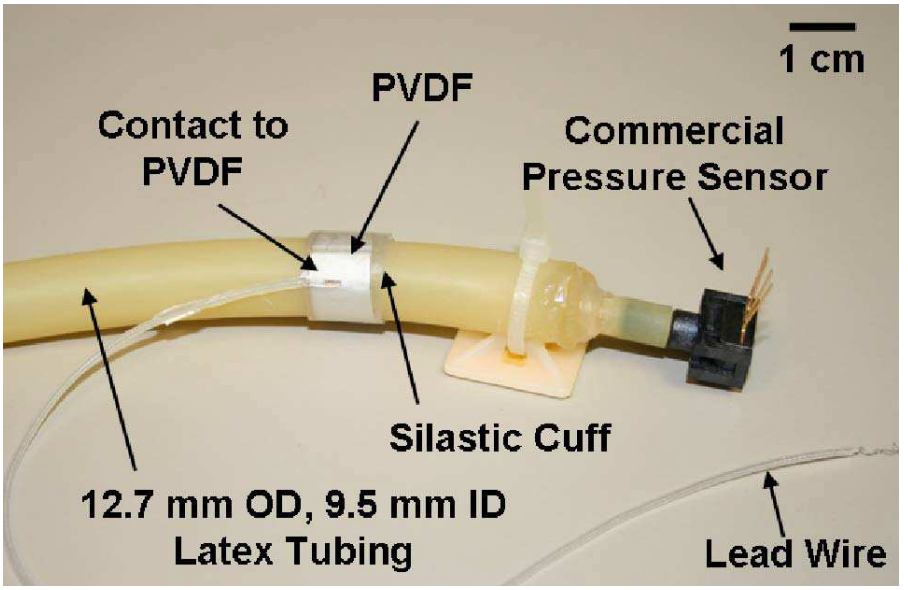

Fig. 2.15 Arterial Cuff Energy harvesterr

An implantable power source (Potkay,2008) that harvests energy from the movements created flow of blood passing in the arteries. The 0.25 cm^2 EH device consists of a piezoelectric film embedded within a flexible, self-curling medical-grade silicone cuff. It is expected to enable self-powered implanted microsystems with increased lifetime, reduced surgical replacement, and minimized external interface requirements compared to its current alternatives. The fabricated device generates up to 16 nW when tested around a mock artery.

2.1.3.3.2 Electromagnetic developed projects and used materials

The most common magnetic material used in electromagnetic EH can be seen Table 2.9 (taken from www.IBSMagnet.com) with their most relevant properties. Being Neodymium-Iron-Boron (NdFeB) of all the permanent magnets the most used, thanks to its high induction and coercivity.

Table 2.9 Magnetic materials and properties

Property	NdFeB	Sm_2Co_{17}	$SmCo_5$
B (mT)	262-278	159-175	143-159
H_c (kA/m)	860-915	636	620
Max operating temp (ºC)	120	300	250
Density (g/cm^3)	7,5	8,4	8,4
Relative permeability	1,37	1,42	1,07

In Table 2.10, some recent electromagnetic human EH systems are shown and then analysed.

Table 2.10 Electromagnetic human EH systems

Source	Frequency (Hz)	Average Power reported(mW)	Ref
Foot motion	1,75	830	(Zeng,2011)
Wrist swing	1.4 to 2.8	0,00361	(Jia,2009)
Walking	2	0,3 0,952	(Saha,2008)
Slow running	2,75	1,86-2,46	(Goudar,2012)

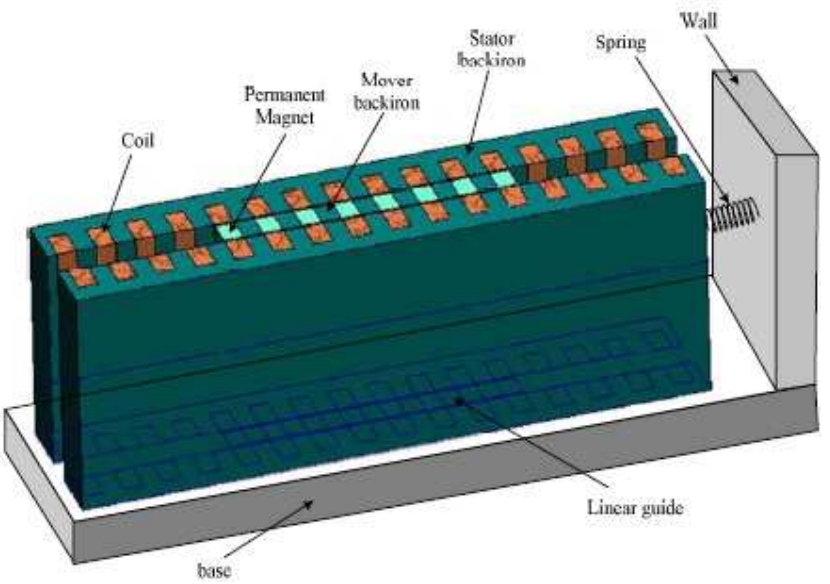

Fig. 2.16 Unconventional electromagnetic energy harvester

One of the greatest prototypes ever made on harvesting the human foot motion is the unconventional electromagnetic energy harvester seen in (Zeng,2011). Instead of using conventionally a coil and a permanent magnet, it uses a translator (Fig. 2.16). That consists of several horizontally magnets with soft magnetic spaces between them. The stator is composed by several in line coils in both sides of the translator to maximize the power output. A spring is connected to a fix platform to provide the sinusoidal movement. A rolling-element with low friction coefficient is placed under the translator to provide a more fluid movement. No other EMVEH researched in this thesis provides a better power output than this system. Using a MPPT (Maximum power point tracking) algorithm regulated for low frequency of foot motion it reaches 830 mW output.

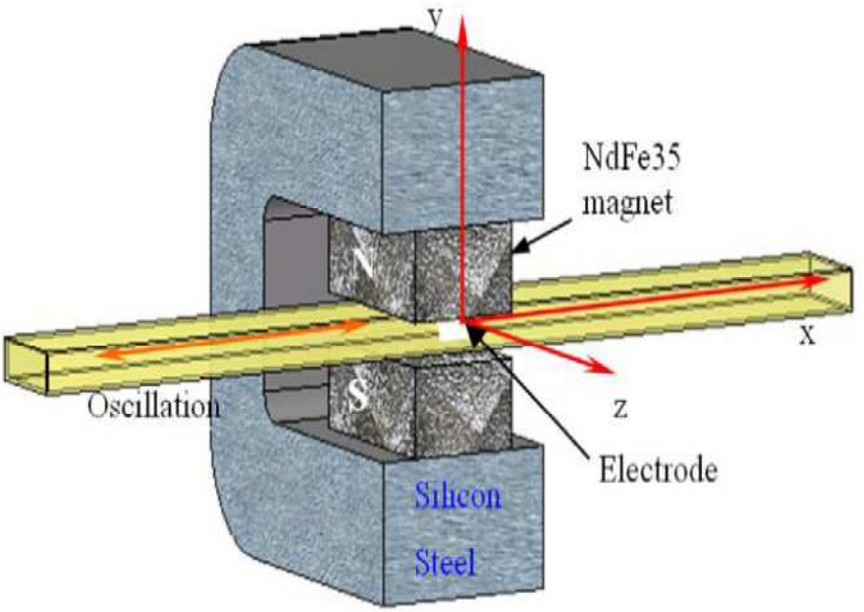

Fig. 2.17 The LMMG

The Liquid Metal Magnetohydrodynamics Generator (LMMG) (Jia,2009) comes with a new concept of flexible energy conversion, adapted to the unpredictable nature of the human movements such as the wrist swing for example. It consists on the electric potential produced when a metal passes through a magnetic field and in this case liquid metal ($Ga_{62}In_{25}Sn_{13}$), to provide the desired flexibility to the converter, rectifying the flow of the material with a plastic valve, but as the previous generators still triggered by an active source of the human body. If we are standing still no power is generated.

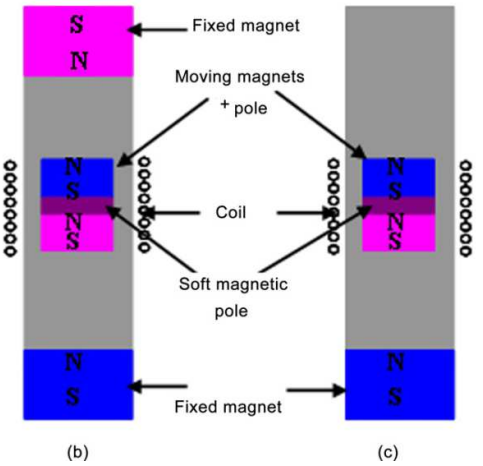

Fig. 2.18 The magnetic spring generator

The magnetic spring generator (Saha,2008) uses the basic principle of electromagnetic conversion to convert the vibration of the human body, using the magnetic field of a permanent magnet that induces voltage in a coil as it passes through it, but with some adjustments, instead

of using a single main magnet, two magnets are glued together separated by a soft pole to increase the linkage flux and instead of a regular spring, a magnetic one is used to increase the vibrations velocity of the main magnet, this magnetic spring is structured by a tube with one or two fix magnets at its extremities, so when the main magnets reaches one of the extremities is repelled to the other end, bouncing between them, or just increasing the speed in one direction if only one fix magnet is used, decreasing the elastic constant but increasing the displacement. The main difficulty faced by this harvester is that a resonant frequency will be hard to achieve due to the low frequency and the lack of steadiness of human motion, and again depend of an active source, once we stop moving the production comes down to zero.

2.1.3.3.3 Electrostatic developed projects and materials

The most common materials used in electrostatic EH are the Electroactive Polymers (EAP) indicated in Table 2.11 with their most relevant properties. The dielectric elastomers (DE) of all the EAP are the most promising material in human energy harvesting. It has an amazing elasticity, matching perfectly human muscles and also a great energy density comparing to other EAP. Comparing to Electrostrictive Polymers (EP) such as (P(VDF-TrFE-CFE) (vinylidene fluoride trifluoroethylene chlorofluoroethylene polymer) to acrylic DE the energy density more than 3 times lower. Regarding integrated electrostatic EH devices based on non EAP, they normally use variable capacitors which are more suitable to machinery vibrations than to human vibration.

Table 2.11 EAP properties (Kornbluh, 2004)

Property	DE		EP			
	acrylic	silicone	(P(VDF-TrFE-CFE)	Graft elastomer	Polyaniline	Polyelectrolyte
Max. strain (%)	380	63	4,5	4	10	>40
Max. pressure (MPa)	8,2	3,0	45	24	450	0,3
Elastic energy density(J/cm^3)	3,4	0,75	1,0	0,48	23	0,06
Max efficiency(%)	60-80	90	n/a	n/a	<1%	30
Relative cycle speed	normal	fast	fast	fast	slow	Slow

In Table 2.12, some recent Electrostatic human EH systems are shown and then further analysed.

Table 2.12 Electrostatic human EH systems

Source	Frequency (Hz)	Average Power reported(mW)	Ref
Footstep	1	200	(Goudar,2012)
Knee rotation	1	0,1[5]	(Jean-Mistral,2008)

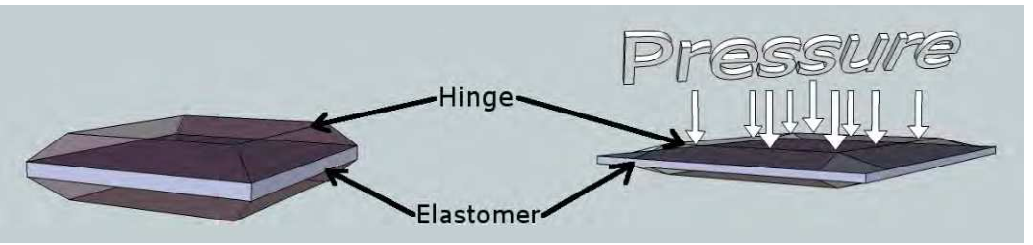

Fig. 2.19 Dielectric elastomer system

DE are deformable polymer films that are built most commonly by acrylics and silicones due to their high elasticity, electric permittivity that is 3 to 10 times greater than the air-gap in electrostatic transducers. Comparing to piezoelectric elements they are much softer and their operational boundaries change when strained, creating the possibility of extracting more energy when stretched. Their high elastic energy density means that with the same quantity of material more energy can be stored, being less obtrusive and more productive transducers, which is very convenient when used in human EH. Being highly elastic materials and not using inertial masses makes them highly efficient working at low frequencies, a characteristic of human motion. In (Goudar,2012) a DE is placed in a shoe insole harvesting the pressure made in each step, being barely noticeable by the user, having 5 times improvement over regular PEGs. The main problem is that it is needs a 2,5 kV charge exactly applied when the pressure reaches is max.

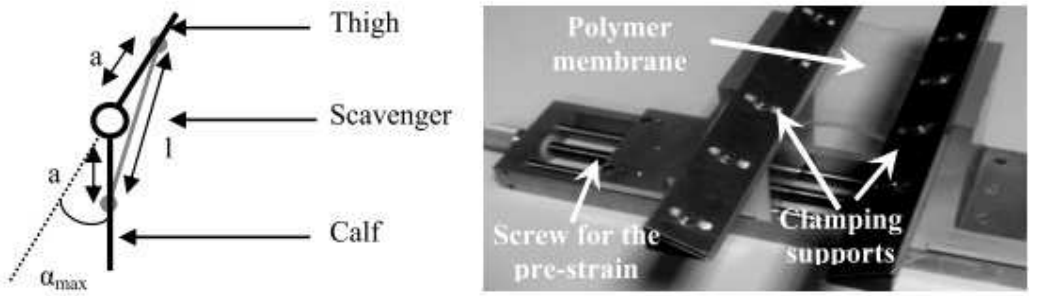

Fig. 2.20 Electrostatic backknee harvester

DE instead of being used under pressure can also be used under strain since their straining ability reaches up to 400%. In (Jean-Mistral,2008) DE is placed in a mechanical scavenger on the back of the knee as we can see in Fig.2.20, the location at the left and the

mechanical scavenger at the right of the picture. Everything the user takes a step it stretches the DE an electrical charge is applied and as the leg comes back energy is generated. This system is very interesting because it actually helps the walking movement. The main problem as all the DE systems is the required high operation voltage.

2.2 CONVERSION TECHNIQUES

All kinds of mechanical energy harvesters, piezoelectric, electromagnetic and electrostatic, are usually employed for the supply of low power electronic devices which require a continuous and stable energy input. Granted that most systems based on the former types of mechanical EH have alternate and unstable outputs, the need for regulation and rectification arises in order to obtain a steady, single polarity voltage, allowing the supply of an electronic device. Such method increases the usable power produced by the harvester.

2.2.1 Basic conversion technique

In order to collect the energy generated by the harvester, the standard approach is to directly connect it to a full rectifying bridge, followed by a filtering capacitor, C_R, smoothing and stabilizing the tension oscillation, as shown in Fig.2.21.

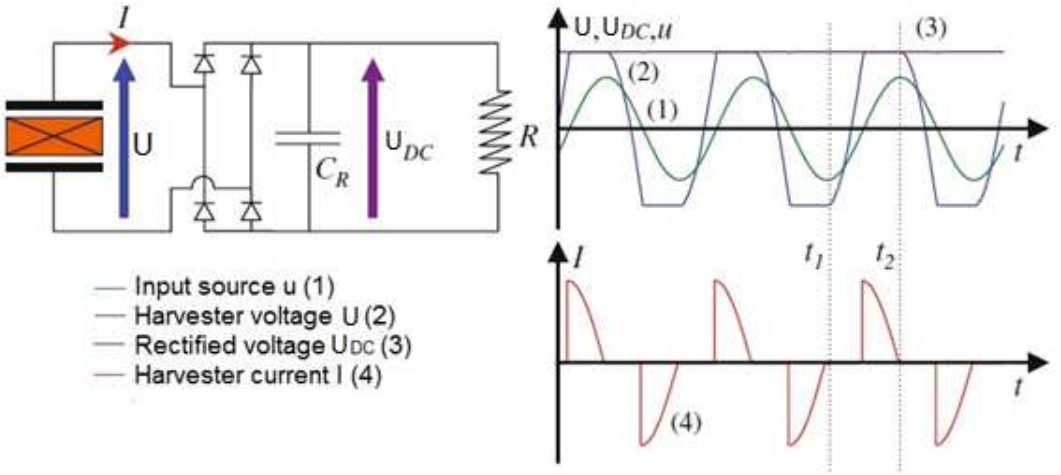

Fig. 2.21 Basic conversion setup and associated waveforms (Inman,2009)

While there is a continuous voltage applied to the load R, the bridge rectifier is blocked when the harvester's voltage U is lower than the rectified voltage U_{DC} in absolute value. The voltage variation is proportional to the strain due to the current I, which exists the piezoelectric elements at a null value. As soon as the voltage U reaches U_{DC}, the bridge rectifier conducts, preventing U from changing. Just as the absolute value of the input source u decreases, the bridge rectifier ceases conducting.

2.2.2 SSHI technique

The synchronized switch harvesting technique (SSHI) technique is similar to the simple conversion technique earlier described with an added a switching system in parallel or in series with the harvester elements. While Fig.2.21 shows the setup and the associated waveforms for the SSHI parallel technique, Fig.2.22 presents the SSHI series technique.

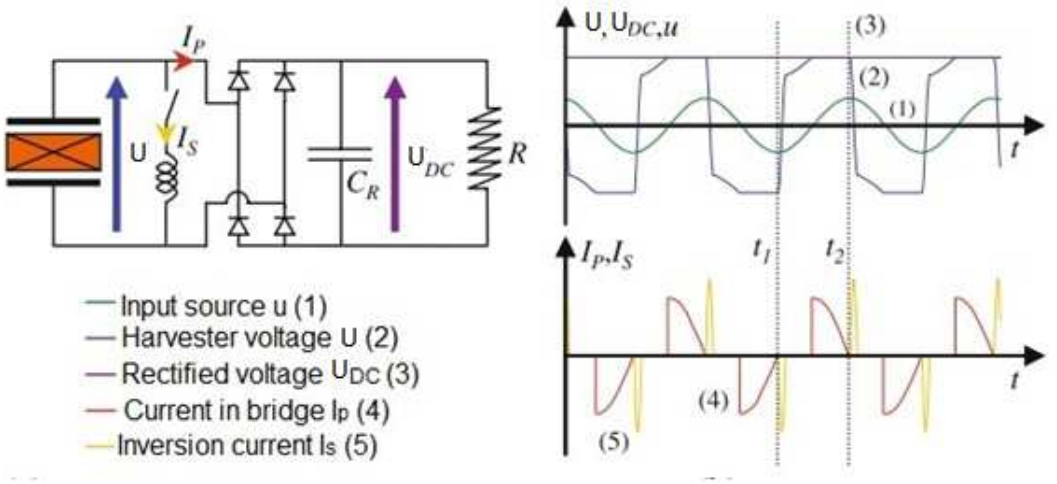

Fig. 2.22 SSHI parallel stetup and associated waveforms (Inman,2009)

The I_P current conducted through the bridge rectifier is null as long as the harvester's voltage U is lower than the rectified voltage U_{DC} in absolute value. The voltage variation is proportional to the displacement. As the absolute value of U equals U_{DC}, the bridge rectifier starts conducting, ceasing the evolution of U. When the displacement u decreases in absolute value, i.e., when a maximum displacement is reached, the bridge rectifier ceases conducting, coinciding with the beginning of the voltage inversion. By annulling the I_P current absorbed by the bridge rectifier leads to the release of the current Is in the inversion inductor.

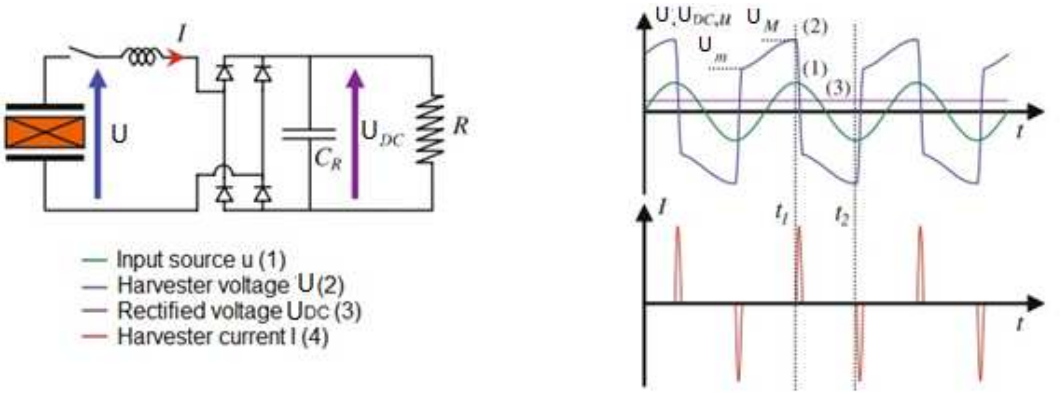

Fig. 2.23 SSHI series stetup and associated waveforms (Inman,2009)

The voltage on the load resistor is continuous in the series SSHI technique configuration. An AC setup of this technique consists in the connection of the load resistance directly in series

with an inversion conductor. The harvester current I is invariably null, the only exception being during the voltage inversion phases. The technique assumes a perfect bridge rectifier as well as a smoothing capacitor Cr large enough to render the voltage U_{DC} constant. Throughout the voltage inversion phases, the voltage at the bridge rectifier input equals $+U_{DC}$ and $-U_{DC}$, when the voltage switches to negative and positive, respectively.

2.2.3 SECE technique

This technique considers a device able to extract energy on the harvester elements within a very brief period of time. Fig.2.23 presents the device applied in the implementation of the Synchronous Electric Charge Extraction (SECE) technique and associated waveforms. In order to bring back the voltage of the piezoelectric elements to zero, their electrostatic energy is extracted at each maximum of displacement. U_M represents the maximum voltage for a positive alternation between instants t_1 and t_2.

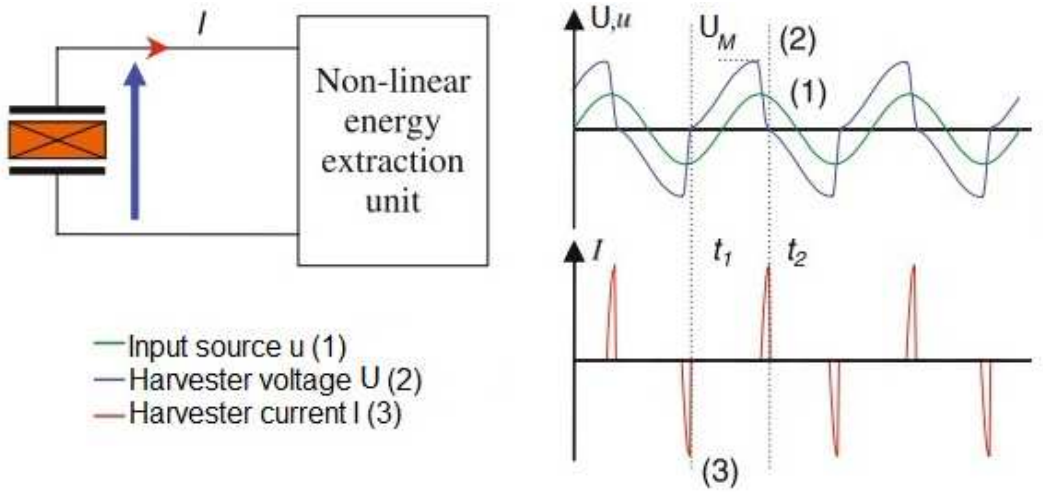

Fig. 2.24 SECE series stetup and associated waveforms (Inman,2009)

The flyback architecture (Fig. 2.24) is one of the possible setups for a load extraction circuit regarding the SECE technique. The voltage gate U_G of the MOSFET (Metal Oxide Semiconductor Field Effect Transistor) transistor T controls this kind of converter. This voltage is determined by a control circuit which detects zeros and maximum peaks of the rectified voltage U_R. Upon reaching a maximum, a voltage of 15V is applied to the transistor gate, setting it to on-state, allowing the transfer to inductance L energy of the harvester elements. As soon as the electric charges presented in the electrodes have been extracted, the control circuit recognizes the cancelation of rectified voltage U_R, thus applying a null voltage to the transistor gate. This operation blocks the transistor, places the harvester elements in open circuit and flows the energy present in the coupled inductor L to the capacitor C_R. The theoretical efficiency of the ideal flyback converter is unitary. The output power therefore equals the input power of the converter and is not a function of the load resistance R, which means the output voltage U_{DC} of

the DC-DC converter is uniquely determined by R. In practice, however, the efficiency of the converter is inevitable imperfect and depends on the load resistance. The power at the converter input is the same as the power extracted from the harvester elements.

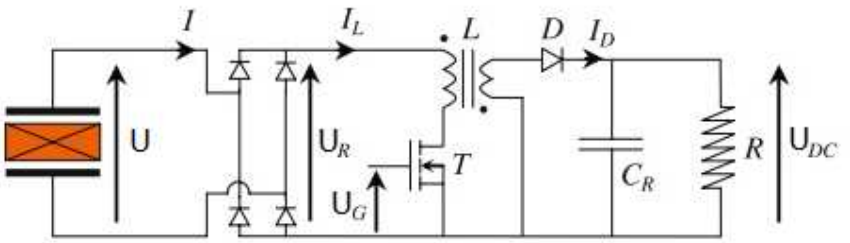

Fig. 2.25 Flyback architecture of a SECE device (Inman,2009)

2.2.4 Comparison of the techniques

The comparison of the four techniques is made through observation of the evolution of the harvested power as a function of the electromechanical figure of merit evolution of the normalized harvested power in comparison to the maximum power harvested with the standard circuit in Fig.2.25. The considered load is chosen to maximize the power supplied by energy harvester in both cases. Depending on the losses of the circuits used for implementing each technique, the series and parallel SSHI may prove better in practice.

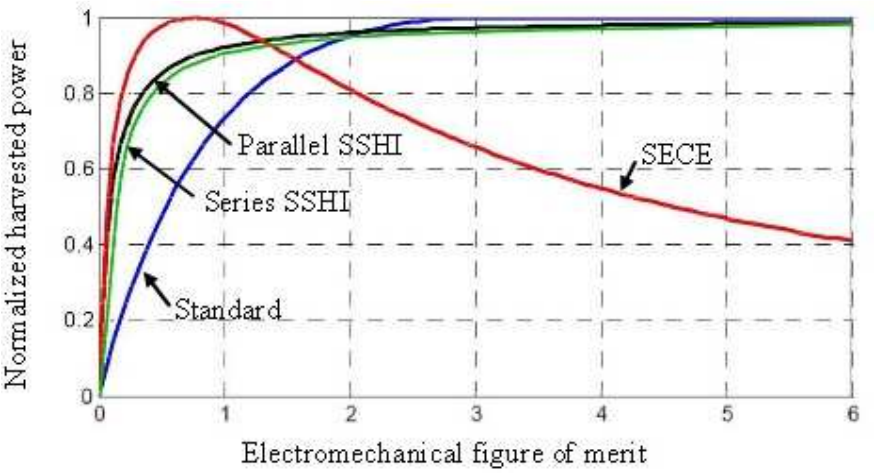

Fig. 2.26 Comparison of the conversion techniques (Inman,2009)

The SECE technique presents itself the most efficient for a low electromechanical figure of merit. Nevertheless, as it increases from approximately 1.4 to 2, the SSHI techniques proves to perform with greater efficiency. After 2, the standard method proves to be the fittest. As so, each technique can be used efficiently depending on the quality of the harvester.

2.3 STORAGE UNIT

There are three possible scenarios of a storage unit in a EH system. First, when the system fully matches the electronic device energy demand, a storage unit won't be necessary. Secondly if the system produces more energy than the device requires but isn't always active, then a battery would be the best choice, so the electronic device can remain active even when the EH system isn't producing energy. When it is producing energy in excess it will be stored in the battery. Or thirdly if the device requires more energy than the EH system can provide but just for brief moments, then a supercapacitor would be the best choice, when the device is offline and the system is producing energy, it can be stored in the supercapacitor and used later when a higher power demand is needed to activate the electronic device.

The main advantages and disadvantages supercapacitors have facing batteries are shown in Table 2.13.

Table 2.13 Supercapacitors versus batteries

Advantages	Almost unlimited life cycles Very fast charging High power density No heat release during discharge No risk of overcharge, maintaining an permitted tension Fast discharges don't have any negative effects Long life time Good behaviour at high temperatures
Disadvantages	Low stored energy density compared to batteries High natural discharge Low max voltage High voltage drop during discharge

When choosing a storage unit for an EH system is very important to first analyse and compare the power source with the power demand of the device that is going to be supplied, only after, a storage unit can be properly chosen. In cases where high power densities are necessary for short intervals supercapacitors are the answer, due their high power density. In situations where a constant voltage is needed for a longer period of time batteries will be the best option.

3 Prototype and its components

A EH device of the human respiration effort was studied and develop taking in consideration the early work of D. Cavalheiro *Breath Energy Transducer*. The developed harvesting device is made of three main elements. A Macro Fiber Composite (MFC) generator is used as the electromechanical transducer of the EH system, a mechanical amplification device which allows the better focus of the low force values of the respiration effort on the MFC and a conversion circuit that rectifies and regulates the input and the output signals of the EH system. In the following sections these three elements will be further analysed.

3.1 MFC GENERATOR

The MFC was invented in 1996 in NASA laboratories, since then it has been object of many studies and tests. In 2002 the manufacturer Smart Material started its production and distribution all over the world. The MFC consist of rectangular, uni-axially aligned piezofibers sandwiched between layers of adhesive and electroded polyimide films. There are two main types of MFC (Fig. 3.1) that use different piezoelectric effects. The P1 type one that uses non-metalized PZT the electric field couples between neighboured finger electrodes of different polarity in the fiber direction (d33 effect) and the P2 type uses PZT fibers with top and bottom electrodes obtained by dicing metalized PZT wafers with all finger electrodes of each side connected together, with the electric field applied through the fiber thickness resulting in a contracting MFC with the advantage of reduced driving voltage (d31 effect) (Cavalheiro,2012).

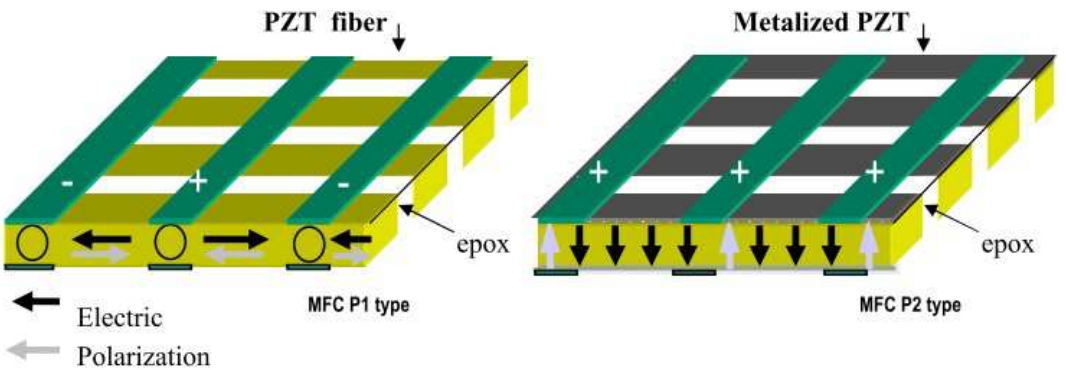

Fig. 3.1 MFC types and element disposition (www.SmartMaterial.com, accessed 03/04/2013)

In Table 3.1 the essential engineering data of the two types of MFC is shown, life tests performed by Smart Material demonstrated that these properties show no significant degradation until 10^{10} cycles. The linear elastic properties are E_{1x}=30 GPa and E_{1y}=16 GPa.

Table 3.1 MFC properties (adapted from www.Smart Material.com)

MFC	Operation voltage		Capacity	Piezoelectric constant		Generator characteristic
	U_{op}^{+}[V]	U_{op}^{-}[V]	C[nF/cm^2]	d_{33}[pC/N]	d_{31}[pC/N]	Charge/Strain[pC/ppm]
MFC P1	1500	-500	0,42	460		1670 [>100V]
MFC P2	360	-60	4,5		-370	3250 [<100V]

Fig. 3.2 MFC P2

3.2 MECHANICAL DEVICE

Analysing previous works done in human respiration effort EH, we can see that the mechanical device works like a link between the movement and the MFC generator, so that input mechanical energy isn't applied directly to the MFC generator protecting it and making it possible to amplify the applied force.

Fig. 3.3 First BET

The mechanical device used in two of the human respiration effort EH projects developed by D. Cavalheiro were analysed. The first can be seen in Fig. 3.3, where a MFC generator is glued to an aluminium bar. The excitation of the MFC is made by straining the aluminium bar, taking in account that the aluminium linear elasticity is 210G Pa, to obtain a certain strain in the MFC a 7 times larger force would have to be applied to the bar. With the small forces involved

in the human respiration the resulting strain would always be very low and insufficient to produce any considerable energy values.

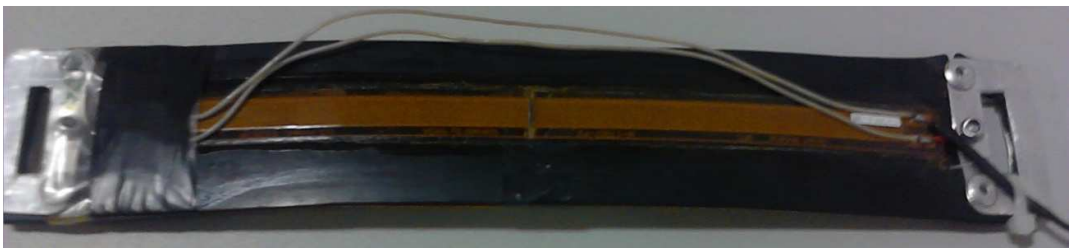

Fig. 3.4 Second BET

On the second device shown in Fig. 3.4, a MFC generator is glued to a rubber support. The excitation of the MFC results by straining the rubber support, taking in account that the rubber linear elasticity is relevantly weaker than the MFC, to obtain a certain strain in the MFC a smaller force could be required. At first glance this phenomenon seems to favour us. But taking in account that the breaking point of the MFC is much smaller than the rubber, this could compromise and damage the piezoelectric material.

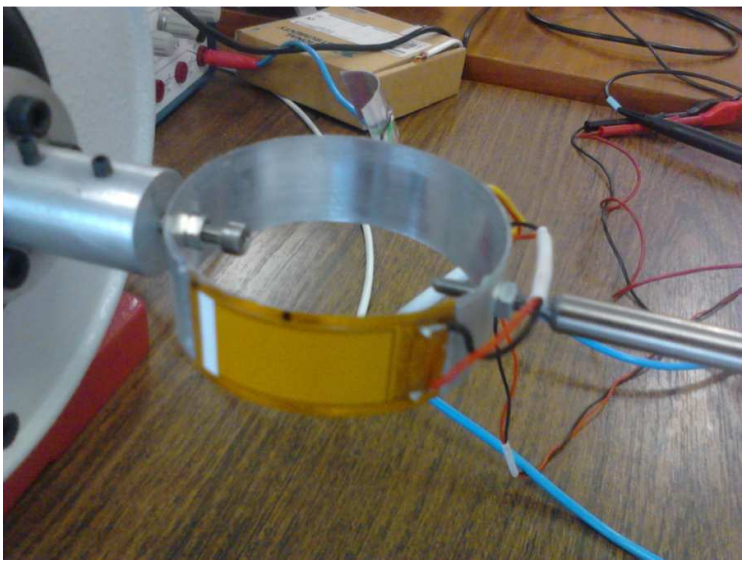

Fig. 3.5 Ring BET

Given the drawbacks of the previous devices, such is the choice for the present mechanical configuration of the harvesting device, Fig. 3.5 and the subject of the following chapter in which the test results are presented. Using a ring mechanical amplification allows us to concentrate the small forces of the human respiration in to the MFC, conserving its integrity.

3.3 CONVERSION CIRCUIT

The mechanical energy cannot be converted completely in electricity due to losses in harvesters. As a rule, the electronic devices must have extremely high efficiency both in energy conversion (harvesters) and energy consumption (the control circuits). Larger losses in the various components are translated into lower conversion efficiencies. To avoid larger losses instead of hand making our own conversion and regulation circuit, the electric matching and the regulation of the output voltage was made by a conditioner module developed by Smart Material called CL-50 (Fig. 3.6).

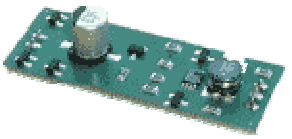

Fig. 3.6 CL-50 Conditioner

It works in a way that it collects the electrical energy developed by the MFC in a first internal buffer stage and once the stored energy reaches a certain level this energy is being passed through a DC voltage regulator circuit to a secondary buffer at the output. This means that a regulated voltage of 3.3V is present at the output until the first buffer stage reaches a critical lower level. When this occurs, the energy transport to the output is stopped until this first buffer is charged up again and the cycle can start again. It's unknown how much energy will collected with the MFC at the applied low frequency movements from the respiratory movement, so maybe it can take several minutes to open the CL50 output for a few ms. As told above this depends on energy balance of harvested energy (from vibration / MFC) and consumed energy (connected load impedance at the output).

4 Experimental procedures

To achieve a better understanding of the human respiratory movement during the breathing process, under different effort levels, a statistic was realised with a group of 30 volunteers. Most of the volunteers were students from UNL-FCT, 19 males with 1,80m and 71 Kg average height and weight and 11 females with 1,66m and 58kg, the average height and weight. In section 4.1 the procedure of the Biopac experiment is presented. And in section 4.2 the procedure and the used components in the prototype experiment are explained.

4.1 BIOPAC EXPERIMENT PROCEDURE

All these experiments were realised in the physics lab of the FCT University, using respiratory effort transducer SS5LB from BIOPAC© attached around the chest voluntary while pedalling in a cycle ergometer (Fig 4.1).

Fig. 4.1 Volunteer performing the test with SS5LB in the cycle ergometer

Measures of the respiratory amplitude and frequency where taken while at different levels of effort, first resting, then with the body producing 50 W and 100 W with the aid of a cycle ergometer and of a heart rate sensor. The SS5LB transducer was connected to the BIOPAC© MP35 measuring system. This system includes data acquisition hardware with built-in universal amplifiers to record and condition electrical signals from the HB. The recorded data then is displayed by numbers as waveforms using Biopac Student Lab software.

The taken steps in the experimental procedure were the following:

-Collecting data of the volunteer: Age, height, weight and gender;

-The heart rate sensor and the SS5LB transducer were sterilized with ethylic alcohol;

-The SS5LB transducer and the heart rate sensor were set on the volunteer as showed in Fig 4.1;

-In the first sample, with the volunteer at rest, the max amplitude, the respiratory frequency and the heart rate were recorded;

-In the second sample, with volunteer producing 50 W using the cycle ergometer, the respiratory frequency and the heart rate were recorded;

-In the third sample, with volunteer producing 100 W using the cycle ergometer, the respiratory frequency and the heart rate are recorded;

4.2 PROTOTYPE EXPERIMENT PROCEDURE

To safely test and calibrate our prototype a series of different equipment was used to emulate the human respiration, instead of implementing it on a person. First using labview and a half-bridge extensometer, Fig. 4.2, a calibration was performed in order to correlate the applied force with the displacement in the material (strain).

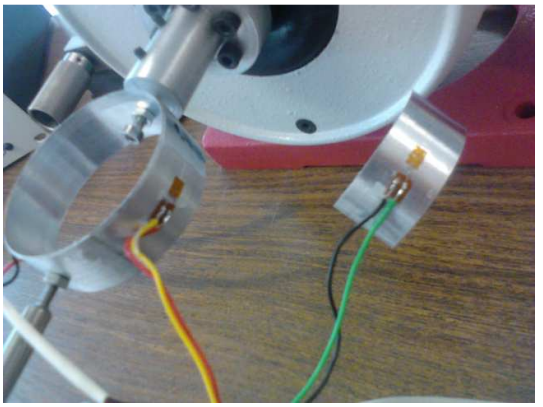

Fig. 4.2 Calibration Set

A frequency generator, Fig. 4.3, was used to ensure the precision of the human respiration average frequencies reached in with the BIOPAC measures.

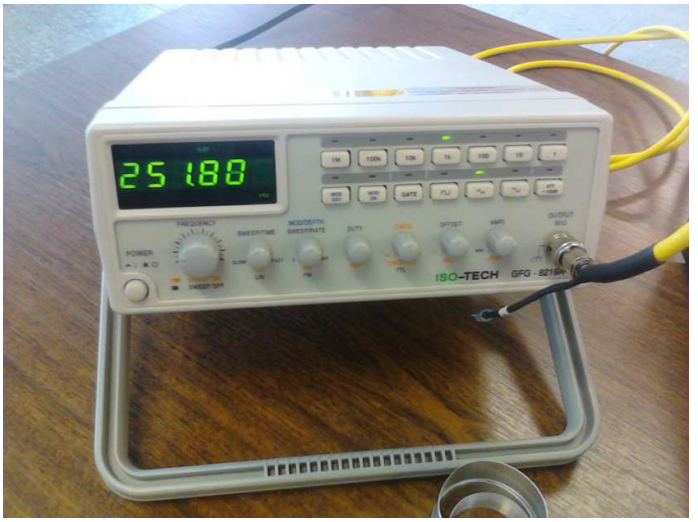

Fig. 4.3 Frequency Generator

To emulate the movement of the human ribs moving during the respiration, the signal created by the frequency generator was fed to a shaker, Fig. 4.4, which is an equipment that replicates vibrations.

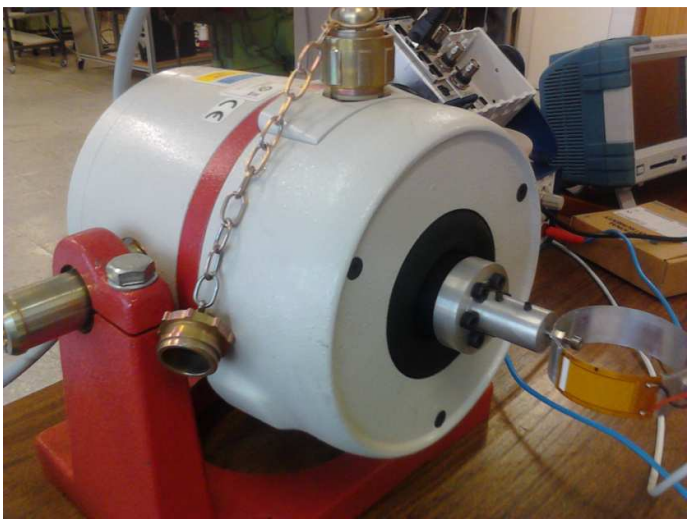

Fig. 4.4 Shaker

The shaker was used to produce movement in the mechanical amplifier exciting the MFC. The movement produced this way was very linear, so it didn't emulate perfectly the human breathing.

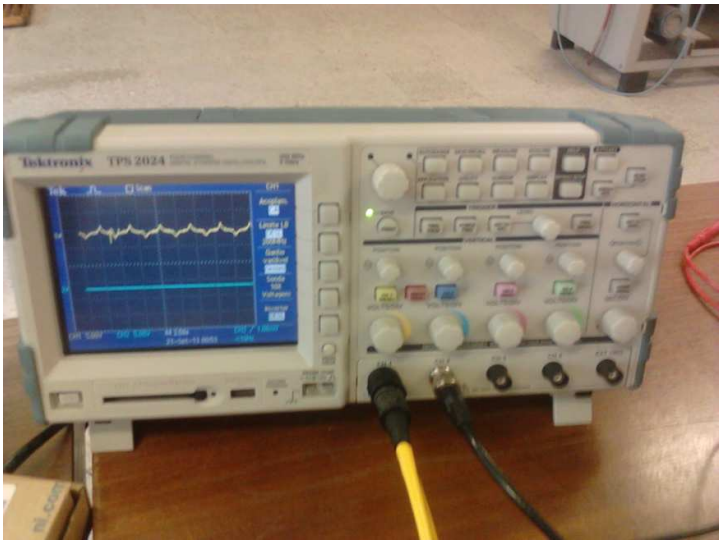

Fig. 4.5 Oscilloscope

To analyse the generated output signals directly from the MFC and with the full circuit an oscilloscope was used, Fig.4.5. For each attempt the outcome was recorded and the values stored for later analysis.

5 Experimental results and analysis

5.1 BIOPAC EXPERIMENT RESULTS AND ANALYSIS

In both genders an increase of the chest expansion was recorded when the effort was increased, as the body needs more oxygen to produce more energy. From the resting state to producing 100 W in the cycle ergometer an average increase of 1,594 cm in male volunteers and 1,051 cm in female, shown in Table 5.1.

Table 5.1 Average chest expansion

	Rest	50 W	100 W
Male	3,126 cm	4,112 cm	4,720 cm
Female	3,191 cm	3,544 cm	4,242 cm

Regarding the frequency of the respiration movement from rest to producing 100 W, it increases from around 1 cycle every 4 seconds to around 2 cycles every 4 seconds, shown in Table 5.2.

Table 5.2 Average respiration frequency

	Rest	50 W	100 W
Male	0,269 Hz	0,421 Hz	0,473 Hz
Female	0,263 Hz	0,430 Hz	0,539 Hz

As predictable as it can be the heart rate increased with the increase of effort.

Table 5.3 Average heart rate

	Rest	50 W	100 W
Male	74-80 bpm	114-122 bpm	135-142 bpm
Female	72-76 bpm	124-129 bpm	145-153 bpm

Through this experiments we reach the conclusion that the work made by the respiration movement increases when the body is in effort. Looking at the frequency changes and taking in account equation (2.5), we can see that energy dissipated by a cyclic movement is directly proportional to the frequency of that movement. So when the body is producing 50 W cycling,

the energy dissipated by the respiration movement increases 1,56 times for men and 1,63 times for woman and when producing 100W, the energy produced increases 1,76 times for men and 2,05 for woman.

5.2 PROTOTYPE EXPERIMENT RESULTS AND ANALYSIS

Using the data collected in the BIOPAC measures from Table 5.1 and 5.2, human respiration movement was emulated through the average between male and female data, Table 5.4. Given an input force (N) created by the shaker and certain strain is produce in the ring mechanical amplifier resulting in a displacement measured by the extensometer. The variation of this strain is what starts the energy production in the MFC, with bigger input forces and faster frequencies the energy production increases.

Table 5.4 Input Frequency and Amplitude

Attempt	1º	2º	3º
Frequency	0,25 Hz	0,4 Hz	0,6 Hz
Amplitude	3,158 cm	3,828 cm	4,481 cm

In each attempt, two voltage outputs were measured using a load range from 1MΩ to 9MΩ. The first directly at MFC terminals before being altered by CL-50 Conditioner, the second after the regulation at the Conditioner terminals.

Achieved values of maximum voltage, Energy per cycle and Joule per second (power) are given in function of a certain load at a given frequency.

5.2.1 First attempt MFC

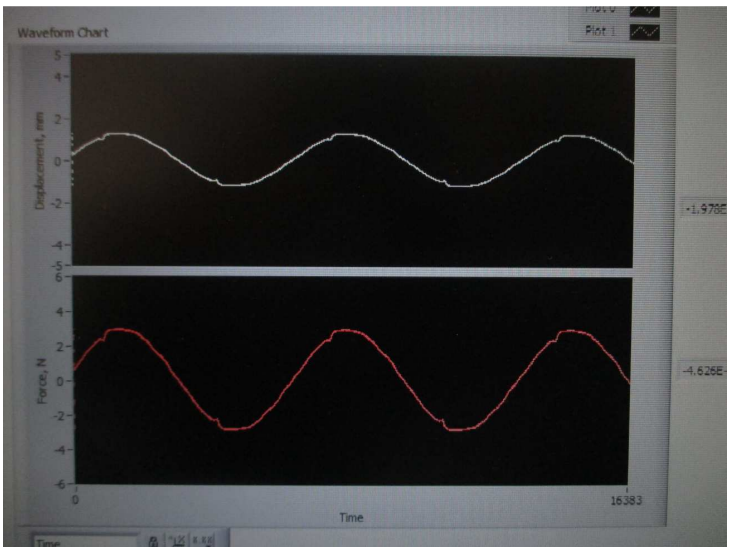

Fig. 5.1 First attempt input signal

In Fig. 5.1 the first attempt is presented, a breathing movement of 0,25 Hz is created emulating an effortless human respiration, with a input force reaching 3,3N resulting in 1,7mm displacement in the mechanical amplifier. The next figures will show all the perform tests at this frequency with load variation.

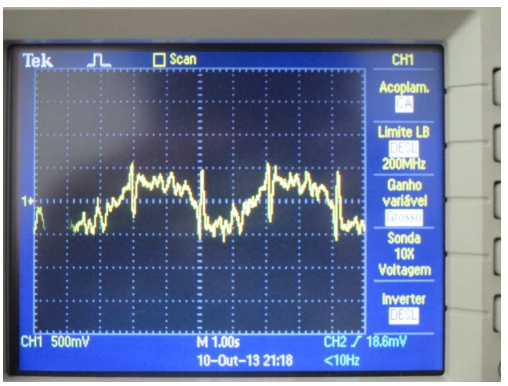

Fig. 5.2 First attempt output with 1MΩ load

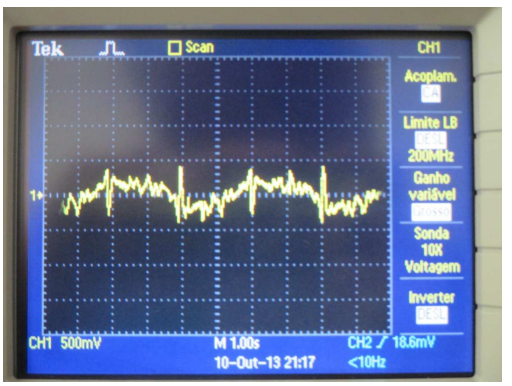

Fig. 5.3 First attempt output with 2MΩ load

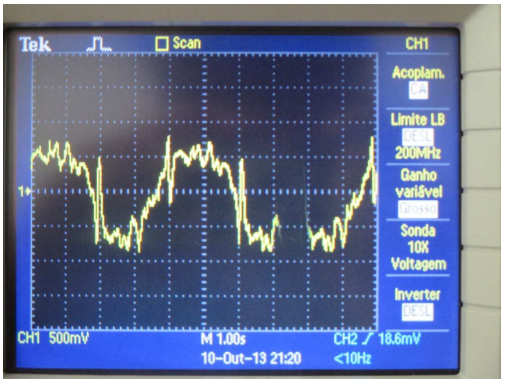

Fig. 5.4 First attempt output with 3MΩ load

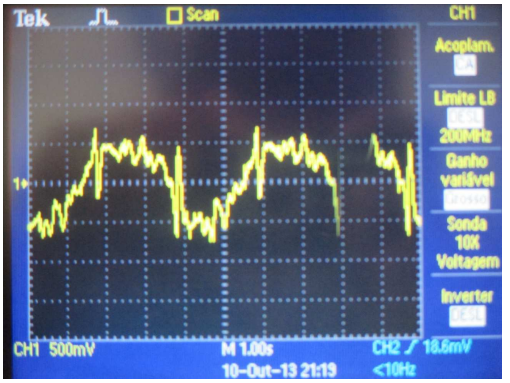

Fig. 5.5 First attempt output with 4MΩ load

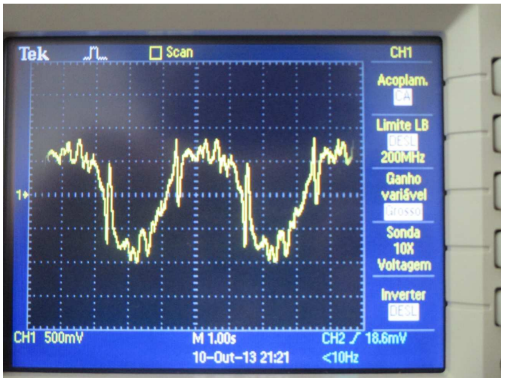

Fig. 5.6 First attempt output with 5MΩ load

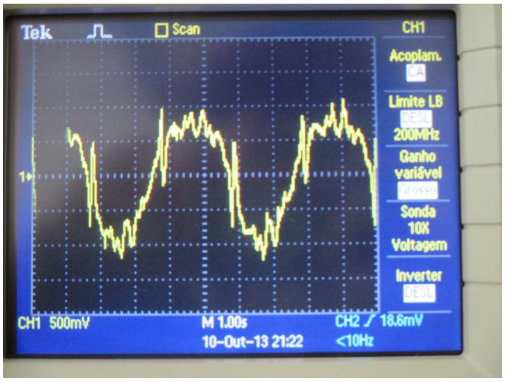

Fig. 5.7 First attempt output with 6MΩ load

Fig. 5.8 First attempt output with 7MΩ load

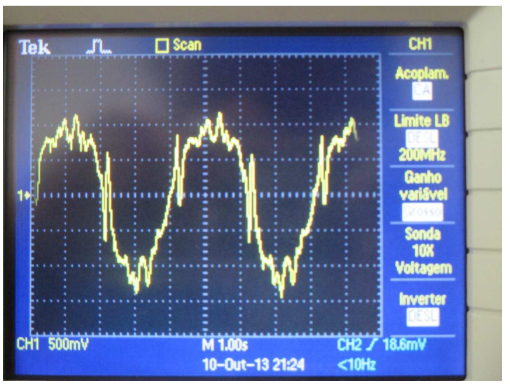

Fig. 5.9 First attempt output with 8MΩ load

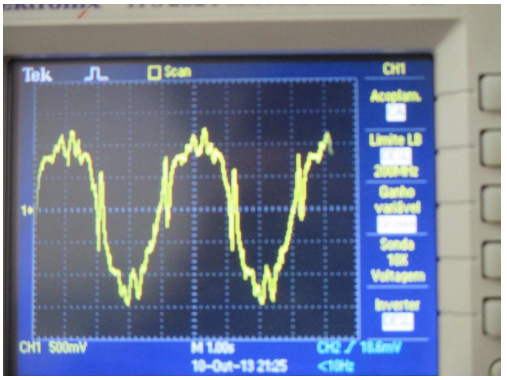

Fig. 5.10 First attempt output with 9MΩ load

Table 5.5 MFC Output at 0,25 Hz

Load (MΩ)	1	2	3	4	5	6	7	8	9
Umax (V)	0,4	0,5	0,7	0,8	0,85	0,9	1,1	1,2	1,3
J/cycle	1,6E-7	1,2E-7	1,6E-7	1,6E-7	1,4E-7	1,3E-7	1,7E-7	1,8E-7	1,8E-7
W	4,0E-8	3,1E-8	4,1E-8	4,0E-8	3,6E-8	3,4E-8	4,3E-8	4,5E-8	4,7E-8

5.2.2 Second attempt MFC

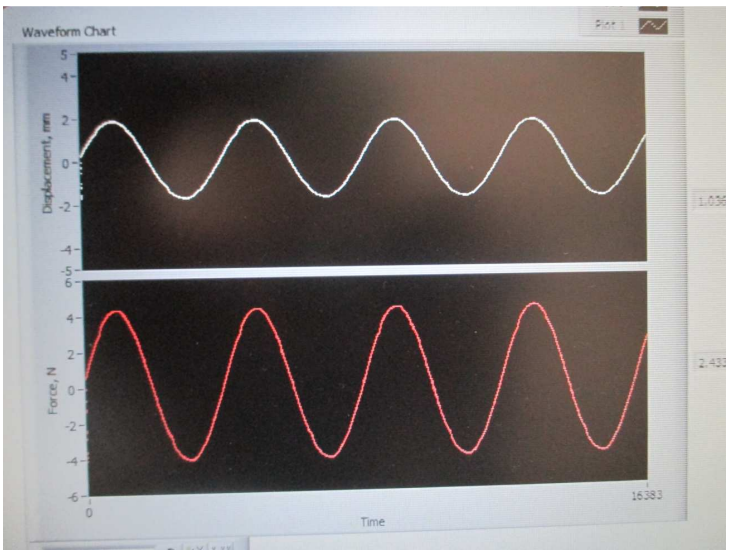

Fig. 5.11 Second attempt input signal

In Fig. 5.11 the second attempt is presented, a breathing movement of 0,4 Hz is created emulating a more accelerated human respiration, with a input force reaching 4,2N resulting in 1,9mm displacement in the mechanical amplifier. The next figures will show all the perform tests at this frequency with load variation.

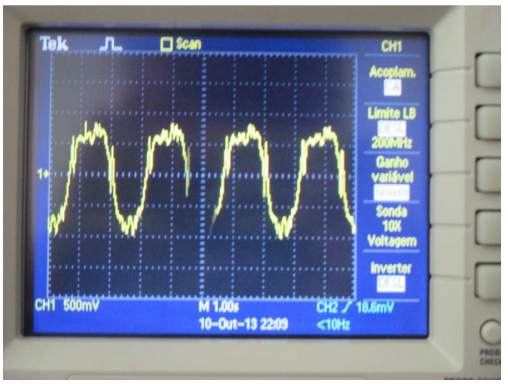

Fig. 5.12 Second attempt output with 1MΩ load

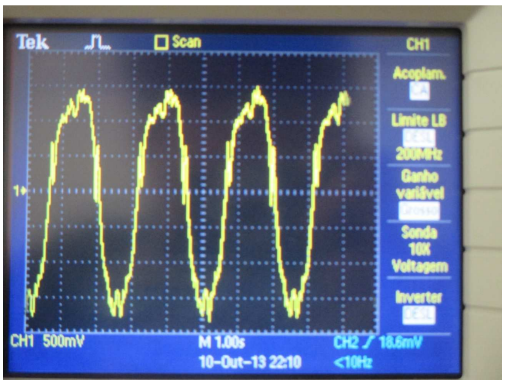

Fig. 5.13 Second attempt output with 2MΩ load

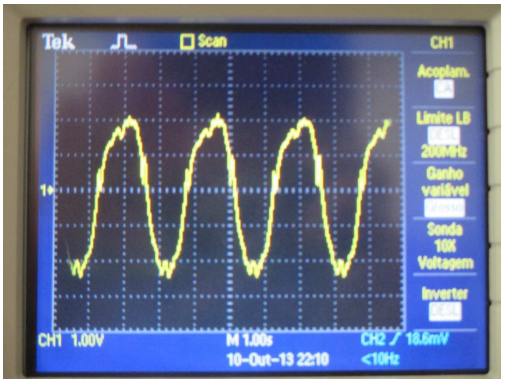

Fig. 5.14 Second attempt output with 3MΩ load

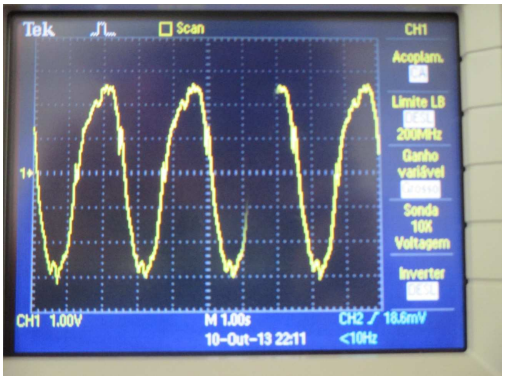

Fig. 5.15 Second attempt output with 4MΩ load

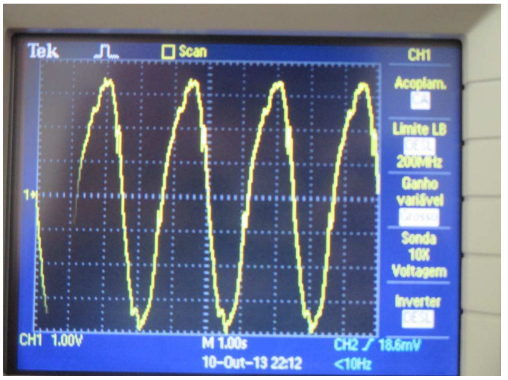

Fig. 5.16 Second attempt output with 5MΩ load

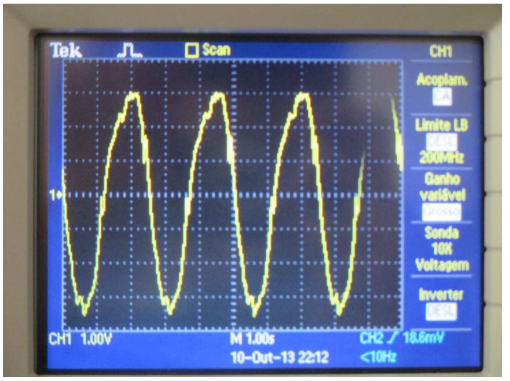

Fig. 5.17 Second attempt output with 6MΩ load

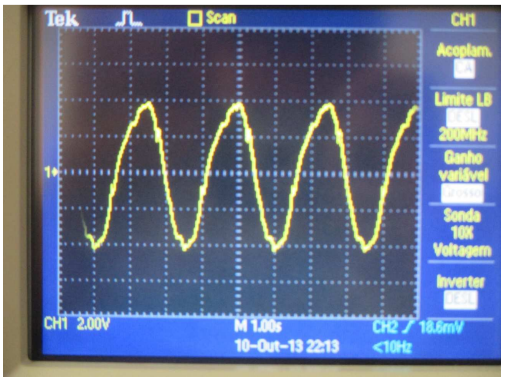

Fig. 5.18 Second attempt output with 7MΩ load

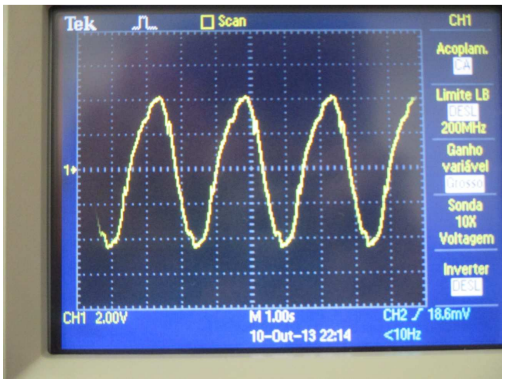

Fig. 5.19 Second attempt output with 8MΩ load

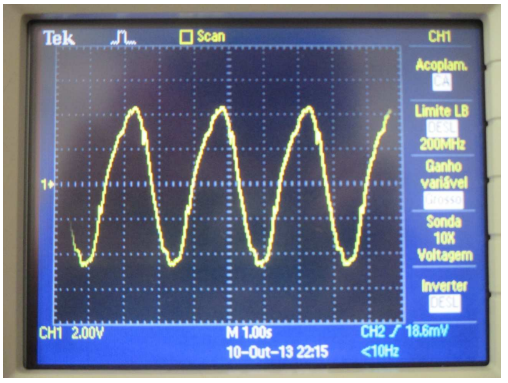

Fig. 5.20 Second attempt output with 9MΩ load

Table 5.6 MFC Output at 0,4 Hz

Load (MΩ)	1	2	3	4	5	6	7	8	9
Umax (V)	0,8	1,5	2	2,6	3	3,4	3,8	4,2	4,5
J/cycle	6,4E-7	1,1E-6	1,3E-6	1,7E-6	1,8E-6	1,9E-6	2,1E-6	2,2E-6	2,3E-6
W	2,6E-7	4,5E-7	5,3E-7	6,8E-7	7,2E-7	7,7E-7	8,2E-7	8,8E-7	9,0E-7

5.2.3 Third attempt MFC

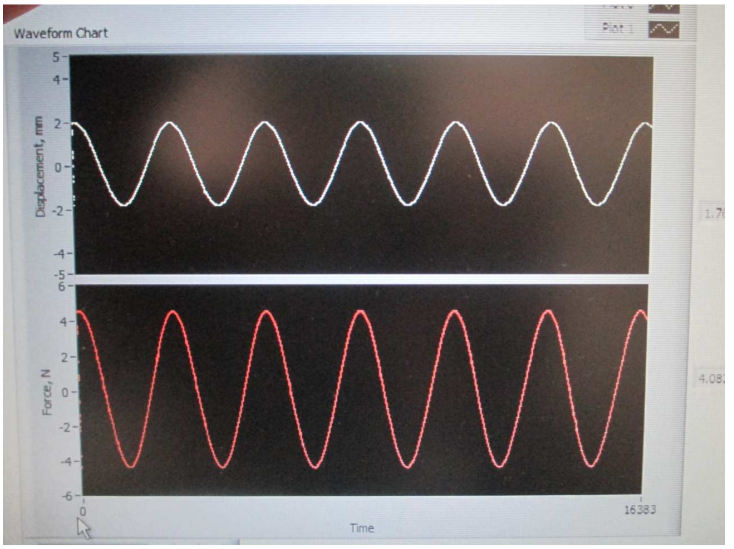

Fig. 5.21 Third attempt input signal

In Fig.21 the third attempt is presented, a breathing movement of 0,6 Hz is created emulating a highly accelerated human respiration, with a input force reaching 4,7N resulting in 2mm displacement in the mechanical amplifier. The next figures will show all the perform tests at this frequency with load variation.

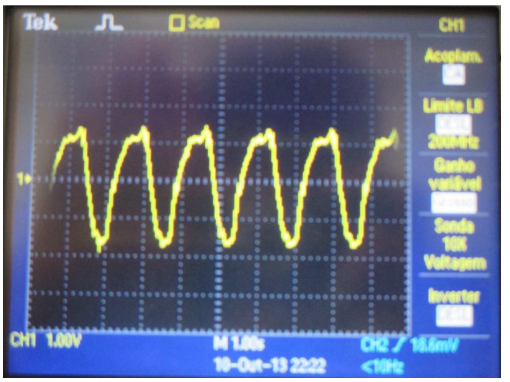

Fig. 5.22 Third attempt output with 1MΩ load

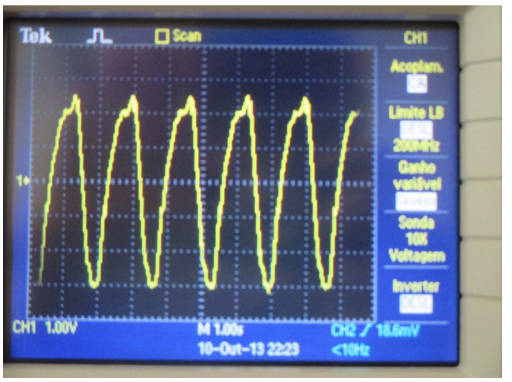

Fig. 5.23 Third attempt output with 2MΩ load

Fig. 5.24 Third attempt output with 3MΩ load

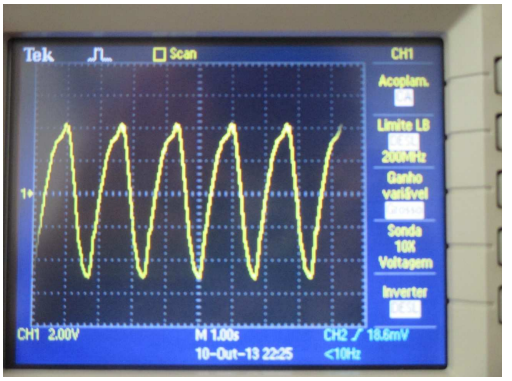

Fig. 5.25 Third attempt output with 4MΩ load

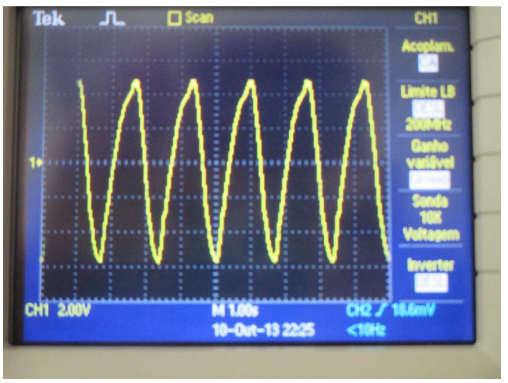

Fig. 5.26 Third attempt output with 5MΩ load

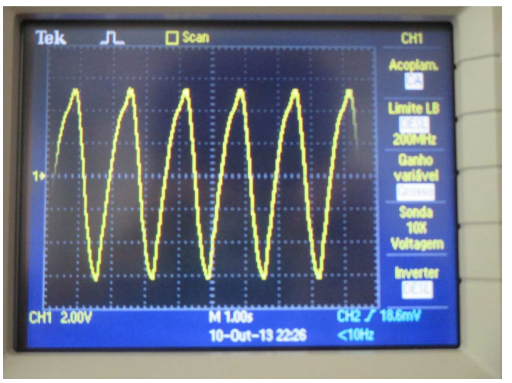

Fig. 5.27 Third attempt output with 6MΩ load

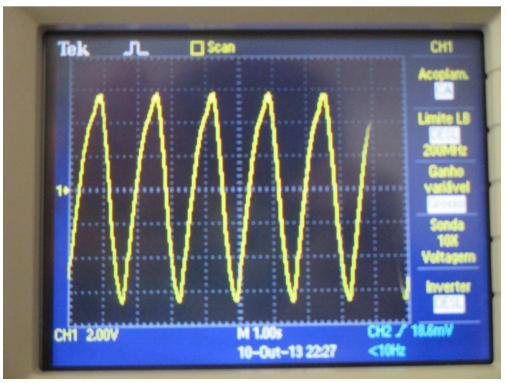

Fig. 5.28 Third attempt output with 7MΩ load

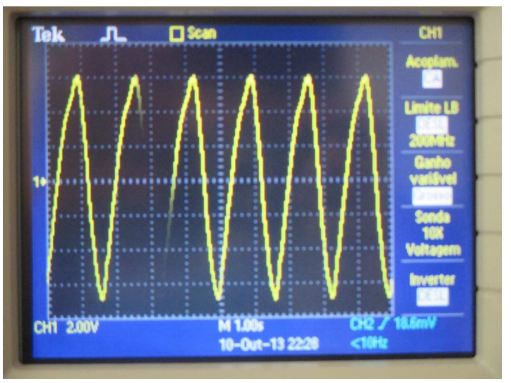

Fig. 5.29 Third attempt output with 8MΩ load

Fig. 5.30 Third attempt output with 9MΩ load

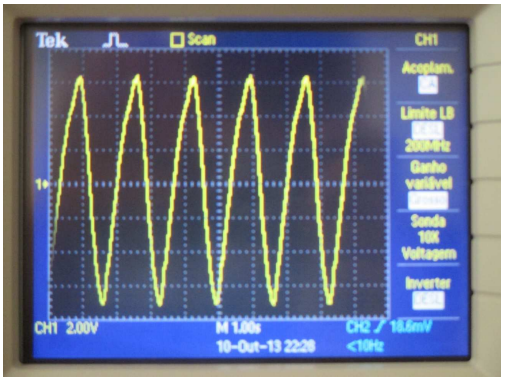

Table 5.7 MFC Output at 0,6 Hz

Table 5.8 MFC Output at 0,6 Hz

Load (MΩ)	1	2	3	4	5	6	7	8	9
Umax (V)	1,2	2,4	3,4	4,2	4,8	5,2	5,8	6	6,4
J/cycle	1,4E-6	2,9E-6	3,8E-6	4,4E-6	4,6E-6	4,5E-6	4,8E-6	4,5E-6	4,5E-6
W	8,6E-7	1,7E-6	2,3E-6	2,6E-6	2,8E-6	2,7E-6	2,9E-6	2,7E-6	2,7E-6

5.2.4 MFC attempt comparison

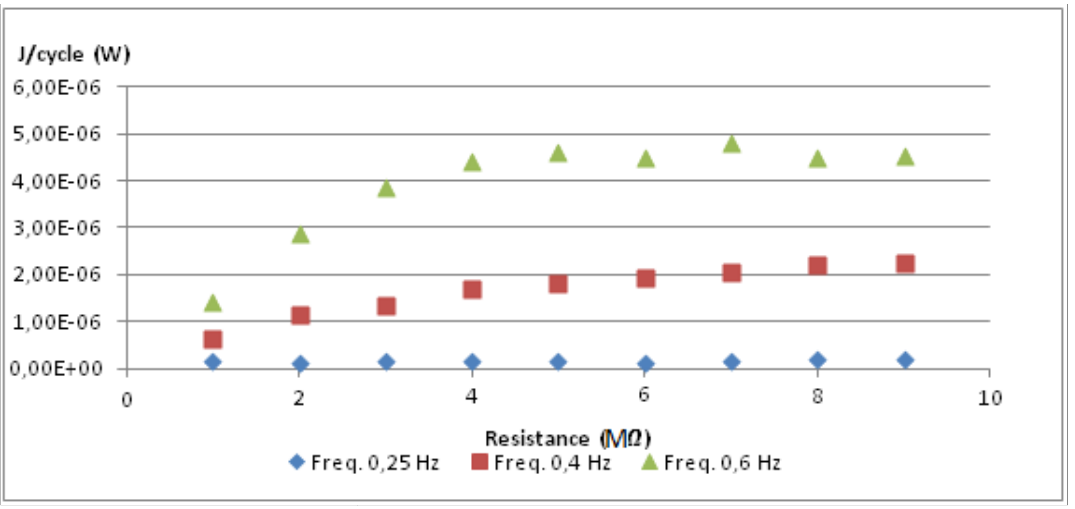

Fig. 5.31 Comparison of the MFC outputs

Using the equation (2.15) provided in chapter 2, the energy dissipated in the load can be calculated by using the square of the rms voltage divided by the resistance of the load. Providing the possible energy to be harvested by the CI-50.

In Fig. 5.31, a comparing all the samples we can conclude that the load matching for maximum energy output is reached with 7MΩ at a frequency of 0,6Hz, resulting in almost 5 µJ/cycle.

5.2.5 Cl-50 attempts and analysis

Due to the redundancy of the null achieved results of the CL-50 outputs, only Fig.5.32 is presented.

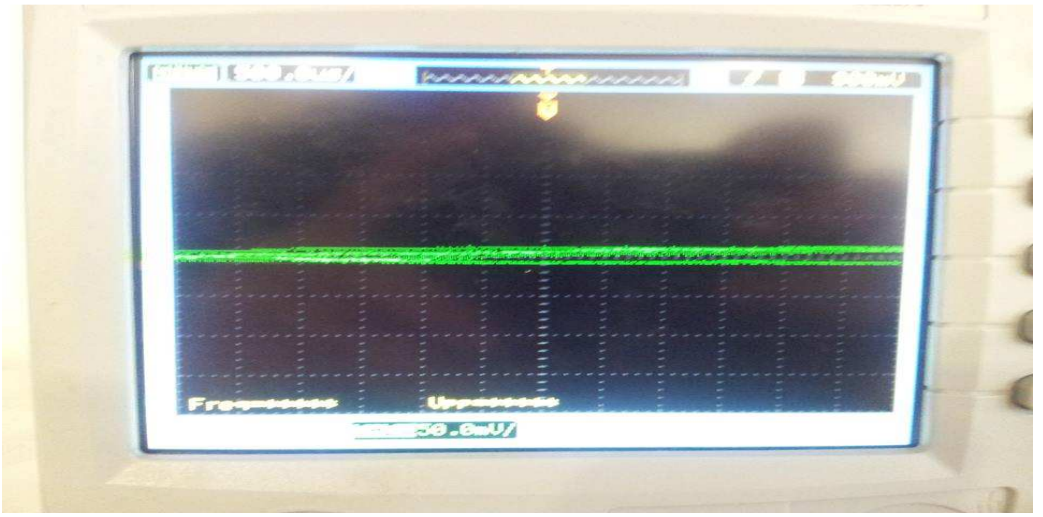

Fig. 5.32 Cl-50 attempts output

Table 5.9 Cl-50 Output at 0,25 Hz

Load (MΩ)	1	2	3	4	5	6	7	8	9
Umax (V)	0	0	0	0	0	0	0	0	0
J/cycle	0	0	0	0	0	0	0	0	0
W	0	0	0	0	0	0	0	0	0

Table 5.10 Cl-50 Output at 0,4 Hz

Load (MΩ)	1	2	3	4	5	6	7	8	9
Umax (V)	0	0	0	0	0	0	0	0	0
J/cycle	0	0	0	0	0	0	0	0	0
W	0	0	0	0	0	0	0	0	0

Table 5.11 Cl-50 Output at 0,6 Hz

Load (MΩ)	1	2	3	4	5	6	7	8	9
Umax (V)	0	0	0	0	0	0	0	0	0
J/cycle	0	0	0	0	0	0	0	0	0
W	0	0	0	0	0	0	0	0	0

6 Conclusions and Future Work

6.1 CONCLUSIONS

Given the obtained results in chapter 5, we can assume that the Cl-50 Conditioner internal circuits consumed all of the energy produced by the MFC generator. Which was almost 5 µJ/cycle with 7MΩ load and a 0,6HZ input frequency.

To debug this occurrence, inhuman respiration frequencies of 5 Hz and 10 Hz were simulated with the shaker, but the output of Cl-50 was still inexistent.

A different conditioner from Linear Technology (Fig. 6.1) with assumed lower internal resistance was also tested but the null output maintained.

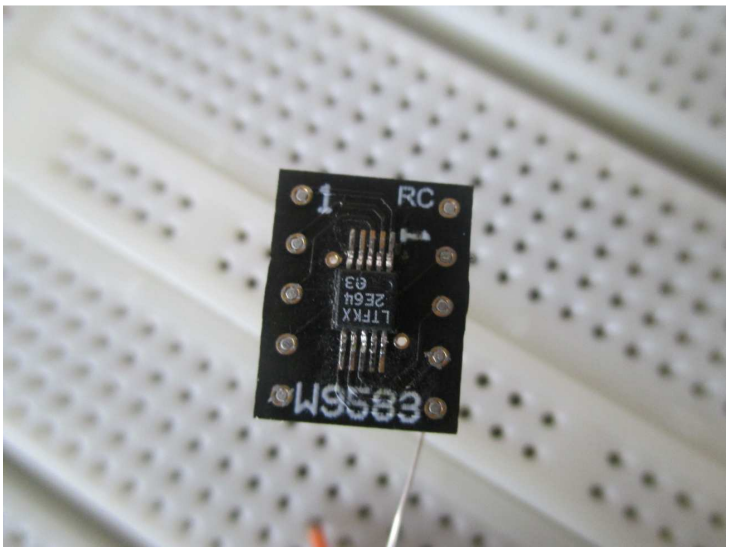

Fig. 6.1 Linear Technology conditioner

There some points that must be considered in the experiments, which are mainly that to achieve more realistic results, more realist data has to be used. For example in the Biopack breathing effort simulation experiment the ages of the volunteers are not in the same range. This distorts the final results. Also the shaker produces very linear vibration movements which are not at all comparable with the human breathing. This also influences noticeably the final results.

In general, the objectives of this dissertation were completed. Even though the results were almost all null, future workers on this subject may use this project has a guide. Taking different and more realist approaches on generating energy by scavenging the human breathing effort.

6.2 FUTURE WORK

A possible future work of this project may consist in adding multiple MFC generators to the mechanical amplifier, in order to increase the power input on the used conditioner. So the power demand of the conditioner is fulfilled and a steady and stable output is created at its terminals.

Other possible way to increase the energy production of the MFC generator is to create a mechanism that is able greatly enhance the low frequencies of the human breathing by using some sort of spring like mechanism. Or even a lever like mechanism, transforming the small forces of the human breath in much more intense and focused inputs.

In a future work if any statistical experiment is performed it should be more realistic. Different groups of similar ages could be created and perform several independent tests. In order to achieve more trustful data, so that more trustful results are produced.

Also regarding the use of more close to the reality results, instead of using machinery like shakers and frequency generators, maybe the tests could be made directly which the HB, granting us a better understanding of possibilities in harvesting this infinite source of energy that is the HB.

I believed that but adding such modifications to this prototype and using these different experimental approaches, enough power would be generated to supply any low power electrical device for a life time or until the user stops breathing.

References

*(Donelan,2009) Donelan, J.M., Naing, V. & Li, Q., 2009. Biomechanical EH. 2009 IEEE Radio and Wireless Symposium, pp.1–4.

*(Riemer,2011) Riemer, R. & Shapiro, A., 2011. Biomechanical energy harvesting from human motion: theory, state of the art, design guidelines, and future directions. Journal of neuroengineering and rehabilitation, 8(22).

*(Starner,2004) Starner, T. & Paradiso, J., 2004. Human generated power for mobile electronics. Low-power electronics design.

*(Tsai,2012) Sue, C. & Tsai, N., 2012. Human powered MEMS-based energy harvest devices. Applied Energy, 93, pp.390–403.

*(Leonov,2013) Leonov, V., 2013. Thermoelectric Energy Harvesting of Human Body Heat for Wearable Sensors. IEEE Sensors Journal, 13(6), pp.2284–2291.

*(Wang,2007) Wang, Z. & Leonov, V., 2007. Micromachined thermopiles for energy scavenging on human body. Tranducers & Eurosensors '07, pp.911–914.

*(Cottone,2012) Cottone, F., 2012. Introduction to vibration energy harvesting. Marie Curie Research Fellow

*(Meng,2006) Meng, Q., Li, B. & Holstein, H., 2006. Recognition of human periodic movements from unstructured information using a motion-based frequency domain approach. Image and Vision Computing, 24(8), pp.795–809.

*(Mitcheson,2010) Mitcheson, P.D., 2010. Energy harvesting for human wearable and implantable bio-sensors. IEEE Engineering in Medicine and Biology Society. Conference, pp.3432–3436.

*(Tan,2011) Tan, Y.K., 2011., Sustainable Energy Harvesting Technologies-Past, Present and Future, InTech.

*(Mateu,2005) Mateu, L. & Moll, F., 2005. Review of energy harvesting techniques and applications for microelectronics.

*(Inman,2009) Inman, D. J. e Priya, S. 2009. Energy Harvesting Technologies. Virginia Tech Center for Intelligent Material Systems and Structures, USA.

*(Howells,2009) Howells, C. a, 2009. Piezoelectric energy harvesting. Energy Conversion and Management, 50(7), pp.1847–1850.

*(Klimiec,2008) Klimiec, E. et al., 2008. Piezoelectric polymer films as power converters for human powered electronics. Microelectronics Reliability, 48(6), pp.897–901.

*(Feenstra,2008) Feenstra, J., Granstrom, J. & Sodano, H., 2008. Energy harvesting through a backpack employing a mechanically amplified piezoelectric stack. Mechanical Systems and Signal Processing, 22(3), pp.721–734.

*(Potkay,2008) Potkay, J. A., Ph, D., & Brooks, K., 2008. An Arterial Cuff Energy Scavenger For Implanted Microsystems, 1580–1583.

*(Zeng,2011) Zeng, P. et al., 2011. Unconventional Wearable Energy Harvesting from Human Horizontal Foot Motion. , pp.258–264.

*(Jia,2009) Jia, D., Liu, J. & Zhou, Y., 2009. Harvesting human kinematical energy based on liquid metal magnetohydrodynamics. Physics Letters A, 373(15), pp.1305–1309

*(Saha,2008) Saha, C.R. et al., 2008. Electromagnetic generator for harvesting energy from human motion. Sensors and Actuators A: Physical, 147(1), pp.248–253.

*(Goudar,2012) Goudar, V. & Potkonjak, M., 2012. Dielectric Elastomer Generators for Foot Plantar Pressure Based Energy Scavenging. , pp.1–4.

*(Jean-Mistral,2008) Jean-Mistral, C., Basrour, S. & Chaillout, J.-J., 2008. Dielectric polymer: scavenging energy from human motion Y. Bar-Cohen, ed. , 6927(692716), pp.1–10.

*(Cavalheiro,2012) Cavalheiro, D., Silva, A. & Valtchev, S., 2012. Energy Harvested from Respiratory Effort

*(Kunzmann,2009) Daue, T.P., Kunzmann, J. & Schönecker, A., 2009 Energy Harvesting systems using piezo-electric Macro Fiber Composites

*(Starner,1971) Angrist, S. W. (1971) "Direct energy conversion", Allyn and Bacon, Inc. USA.

*(Lallart,2012) Lallart, M. ed., (2012). Small-Scale Energy Harvesting, InTech

*(Mateu,2009) Sáez, M. & Loreto, M., (2009). Energy harvesting from human passive power. Universitat Politécnica de Catalunya.

*(Inman,2009) Inman, D. J. & Priya, S. (2009). Energy Harvesting Technologies. Virginia Tech Center for Intelligent Material Systems and Structures, USA.

*(S.Roundy,2003) Roundy S.J. (2003) Energy Scavenging for Wireless Sensor Nodes with a Focus on Vibration to Electricity Conversion. University of California.

*(Kornbluh,2004) Kornbluh, R. (2004). Electroactive polymers : An emerging technology for MEMS, 5344, 13–27.

Appendix

BIOPAC MALE USER DATA TABLES

Name	Age	gender	height	weight
Pawel	23	M	1,71	64
Razvan	21	M	1,75	65
Cris	23	M	1,88	85
Miguel	23	M	1,82	71
Hugo	24	M	1,72	62
Duarte	26	M	1,81	79
Diogo	25	M	1,78	103
Pedro Spain	22	M	1,85	78
Pedro Cartaxo	26	M	1,68	70
Diogo Soares	24	M	1,76	84
Lucas Valadares	19	M	1,81	70
Francisco Costa	20	M	1,78	58
Pedro Soares	24	M	1,8	82
Alexandre Moura	26	M	1,81	84
Diogo Quadros	24	M	1,73	60
Pedro Amaral	24	M	1,82	71
Fabio Cardona	27	M	1,83	74
João Macau	22	M	1,8	77
Miguel Alves	23	M	1,82	68
André Brigida	24	M	1,71	61
Sergio Brigida	21	M	1,72	63
Average	24		1,8	71

BIOPAC FEMALE USER DATA TABLES

Name	Age	gender	height	weight
Maria	21	F	1,62	50
Diana Machado	22	F	1,7	61
Sara Matos	20	F	1,72	54
Catarina Silva	27	F	1,6	63
Diana Machado	22	F	1,7	61
Sara Matos	20	F	1,72	54
Catarina Silva	27	F	1,6	63
Claudia Ralo	25	F	1,67	55
Joana Carreira	25	F	1,65	55
Andreia Carvalho	23	F	1,52	70
Joana Almeida	26	F	1,61	47
Ana Rita	21	F	1,69	55
Teresa Januaria	54	F	1,67	72
Maria Antónia	59	F	1,58	87
Average	24		1,66	58

BIOPAC MALE PERFORMANCE DATA TABLES

	Repouso (s)	Bpm(pulse/min)	time	Bpm	time	Bpm	rest min(mv)	rest max(mv)	rest amp(mv)	rest freq(mv)	50w min(mv)	50w max(mv)	50w amp(mv)	50w freq(mv)	100w min(mv)	100w max(mv)	100w amp	100w freq
Pawel	0-44	80-85	44-72	110-114	72-120	137-140	-3,3	1,8	5,2	0,3	-4,6	6,4	11,0	0,5	-4,3	7,4	11,6	0,6
Razvan	0-30	80-85	30-60	120-126	60-80	143-149	-1,9	4,5	6,4	0,3	-4,2	6,0	10,1	0,4	-4,2	5,8	9,9	0,5
Miguel	0-36	72-75	36-80	115 120	80-136	130-142	-1,8	1,1	2,9	0,4	-3,0	2,3	5,2	0,5	-7,6	3,3	10,9	0,5
Hugo	0-32	83 -85	32-70	116 134	70-136	140-152	-3,2	7,3	10,5	0,3	-5,2	6,3	11,5	0,4	-5,1	7,9	13,0	0,6
Duarte	0-44	72-76	44-74	114-119	74-92	130-142	-2,0	6,1	8,1	0,3	-3,3	7,5	10,8	0,4	-6,1	6,1	12,3	0,3
Diogo	0-20	75 - 80	20-65	106-124	65-94	136-140	-4,1	2,8	6,8	0,3	-8,9	1,8	10,7	0,5	-5,2	4,7	9,9	0,5
Pedro Spain	0-32	72 - 81	32-92	124 - 132	92-132	140-153	-7,3	3,6	10,8	0,2	-9,6	3,1	12,7	0,5	-7,7	2,9	10,6	0,5

Pedro Cartaxo	0-36	75 - 83	36-66	103 - 109	66 - 108	133-143	-3,1	5,4	8,5	0,2	-1,7	8,7	10,5	0,3	-2,6	8,6	11,2	0,3
Diogo Soares	0-27	72-80	27-60	110 -113	60 - 92	135-145	-4,6	6,0	10,6	0,2	-1,4	8,3	9,7	0,5	-4,1	7,5	11,6	0,4
Lucas Valadares	0-38	96 -98	28-70	120-125	70-111	138 - 144	-6,4	6,2	12,6	0,2	-6,7	6,0	12,6	0,6	-7,4	5,5	12,9	0,5
Francisco Costa	0-39	106-108	39-72	146-148	72-110	171-173	4,7	3,2	7,8	0,2	-7,5	2,6	10,0	0,4	-10,5	3,3	13,8	0,6
Pedro Soares	0-30	72-76	30-61	92-96	61-92	100-106	-5,4	4,9	10,2	0,3	-9,9	2,8	12,7	0,4	-11,0	3,0	14,1	0,4
Alexandre Moura	0-31	63-68	31-64	96-98	64-94	116-120	-4,5	3,7	8,2	0,2	-7,0	5,8	12,8	0,4	-7,5	6,3	13,8	0,3
Diogo Quadros	0-33	81-82	33-71	120-127	71-109	152-155	-1,0	0,8	1,7	0,3	-3,7	1,5	5,1	0,3	-7,6	1,8	9,4	0,3
Fabio Cardon	0-33	74-76	33-64	102-105	64-104	124-130	-4,9	4,3	9,1	0,3	-8,0	2,8	10,8	0,3	1,7	11,8	13,4	0,5

a																		
João Macau	0-40	66-68	40-82	96-101	82-136	121-124	-3,4	4,2	7,5	0,3	-5,9	3,7	9,6	0,4	-8,7	3,2	12,0	0,5
Miguel Alves	0-46	81-84	46-95	125-129	95-128	142-146	-3,7	4,6	8,3	0,3	-4,7	5,9	10,6	0,4	-9,0	3,4	12,4	0,5
André Brigida	0-46	53-56	46-112	134-136	112-155	140-143	-5,7	2,6	8,3	0,2	-8,4	4,5	12,9	0,4	-9,3	4,7	13,9	0,5
Sergio Brigida	0-31	61-63	31-83	100-105	83-135	120-124	-3,7	4,8	8,5	0,3	-4,8	5,8	10,5	0,4	-5,6	7,3	12,8	0,5
Average		74,5-80,5		114,5-122		135,5-142,5	-3,4	4,1	8,0	0,3	-5,7	4,8	10,5	0,4	-6,4	5,5	12,1	0,5

BIOPAC FEMALE PERFORMANCE DATA TABLES

	time	Bpm	time	Bpm	time	Bpm	Rest min	Rest max	Rest amp	Rest freq	50w min	50w max	50w amp	50w freq	100w min	100w max	100w amp	100w freq
Maria	0-26	70-73	26-50	120-122	50-75	131-133	-1,1	1,5	2,6	0,2	-6,8	4,1	10,9	0,5	-8,4	4,3	12,7	0,6
Diana Machado	0-30	68-69	30-64	124-126	64-97	141-143	-7,1	7,8	14,8	0,2	-5,3	6,9	12,2	0,6	-6,3	7,7	14,0	0,7
Sara Matos	0-30	60-65	30-61	120-123	61-83	110-112	-3,7	7,7	11,4	0,2	-4,4	6,7	11,1	0,4	-5,6	7,7	13,3	0,5
Catarina Silva	0-33	93-104	30-77	133-136	78-112	156-160	-3,6	4,8	8,4	0,3	-1,5	8,8	10,3	0,5	-4,3	7,5	11,8	0,7
Claudia Ralo	0-31	70-76	31-66	125-129	66-104	145-153	-3,3	3,6	6,9	0,3	-7,0	5,3	12,3	0,4	-9,4	2,8	12,2	0,6
Joana Carreira	0-30	68-72	30-71	123-129	71-105	154-160	-5,4	8,1	13,5	0,3	-3,8	8,7	12,4	0,4	-6,6	7,8	14,4	0,5
Andreia Carvalho	0-32	89-90	32-64	140-144	64-94	166-170	-3,6	2,5	6,1	0,3	-1,8	0,9	2,6	0,3	-3,1	0,9	4,0	0,4
Joana Almeida	0-49	85-86	49-76	139-142	76-100	156-160	-4,9	6,0	11,0	0,3	-6,5	3,6	10,0	0,4	-10,0	4,1	14,1	0,5
Ana Rita	0-32	80-82	32-57	135-140	57-91	155-160	-1,8	0,8	2,6	0,3	-4,1	2,0	6,0	0,4	-9,0	3,1	12,1	0,4
Teresa Januaria	0-32	77-78	32-61	98-100	61-99	110-111	-3,3	2,6	5,9	0,4	-5,0	3,4	8,5	0,4	-7,5	1,7	9,2	0,4
Maria Antónia	0-42	72-74	42-79	111-114	79-121	132-136	-2,7	3,9	6,6	0,2	-2,5	0,9	3,4	0,5	-1,4	0,4	1,8	0,7
Average		72-76		124,5-129		145-153	-3,7	4,5	8,2	0,3	-4,4	4,7	9,1	0,4	-6,5	4,4	10,9	0,5